

Fluoride contamination in groundwater sources in Southwestern Nigeria: Assessment using multivariate statistical approach and human health risk

Order of Authors

1. **Emenike Chidozie PraiseGod*** (praisegod.emenike@covenantuniversity.edu.ng)
¹ Department of Civil Engineering,
Covenant University, Ota, Ogun State, Nigeria

² Cranfield Water Science Institute,
School of Water, Energy and Environment,
Cranfield University, Bedfordshire, United Kingdom.
***(Corresponding author)**
2. **Tenebe Imokhai Theophilus** (imokhai.tenebe@covenantuniversity.edu.ng)
¹ Department of Civil Engineering,
Covenant University, Ota, Ogun State, Nigeria.
3. **Peter Jarvis** (p.jarvis@cranfield.ac.uk)
Professor of Water Science & Technology
² Cranfield Water Science Institute,
School of Water, Energy and Environment,
Cranfield University, Bedfordshire, United Kingdom.

Fluoride contamination in groundwater sources in Southwestern Nigeria: Assessment using multivariate statistical approach and human health risk

Abstract

The present study investigated the ionic and fluoride concentrations in tap water and its associated health risk to local dwellers of Ogun State (Abeokuta south), Nigeria. 63 samples were collected from twenty-one different locations. Results obtained revealed the mean concentration of fluoride (F^-) as 1.23 mg/L. Other water quality parameters such as total dissolved solids (TDS), electrical conductivity (EC), Fe^{2+} , and SO_4^{2-} surpassed the WHO limits for drinking water quality. Strong positive correlation was observed between F^- and TDS; F^- and pH; TDS and EC; TDS and Mg^{2+} ; TDS and SO_4^{2-} ; TDS and HCO_3^- ; EC and HCO_3^- ; EC and SO_4^{2-} ; Na^+ and Cl^- ; SO_4^{2-} and Cl^- . In addition, Empirical Bayesian Kriging (EBK) model was employed to spatially distribute the concentration of the analyzed elements within the study region. The chronic daily dose (CDD) and hazard quotient (HQ) were also used to evaluate the health risk associated with F^- , considering dermal and ingestion as pathways. The results revealed that the associated HQ for infants between the age range of 6–12 months within about 91% of the study region surpassed the accepted HQ limit. However, the HQ for age categories 11–16 years; > 65years; 18–21years; \geq 21years; 16–18years within 95.2%, 90.5%, 80.95% and 100% of the study location were less than 1. Conclusively, the HQ values obtained in this study should serve as a baseline information for water management authorities, policymakers and the society at large towards addressing these pollution issues.

Keywords: Risk assessment; Abeokuta; Pollution; Groundwater; Dispersion; Southwestern Nigeria.

25 **1. Introduction**

26 The presence of fluoride at elevated concentrations in drinking water has caused severe health
27 effects in humans in some parts of the world (Bhatnagar et al., 2011; Shen and Schäfer, 2015).
28 Fluorine exists in the environment through combination with other elements to form highly soluble
29 fluoride compounds. The main source of fluorine in water is from natural deposition from geogenic
30 sources in aquifers (EPA, 2010; Sun et al., 2013). The primary way by which humans ingest
31 fluoride is through consumption of contaminated groundwater (Singh et al., 2013; Singh and
32 Mukherjee, 2015; Subba Rao et al., 2013). The World Health Organization (WHO) recommended
33 the concentration of fluoride that can cause minimal health risk to be 1.5 mg/L. However, more
34 than 200 million people living across 20 developing and developed countries regularly consume
35 water with elevated fluoride concentrations above the standard guidelines set by the WHO (Amini
36 et al., 2008; Fawell et al., 2006; Shen and Schäfer, 2015). Some countries such as Tanzania in the
37 East of Africa have a drinking water standard for fluoride of 4 mg/l, well above the WHO
38 recommended value. This can cause a number of possible health problems, including dental and
39 skeletal fluorosis. In the Rift Valley, East Africa, more than 80 million people display a range of
40 symptoms consistent with dental fluorosis (Shen and Schäfer, 2015; Smedley et al., 2002).
41 However, this should also be placed in the context of water scarcity, population growth and access
42 to clean water in the region.

43 High concentrations of fluoride in humans can lead to various health problems such as nervous
44 system damage (Kaoud and Kalifa, 2010), reduced fertility (Izquierdo-Vega et al., 2008),
45 intellectual impairment in children (Ding et al., 2011; Shivaprakash et al., 2011), urinary tract
46 disease (Jha et al., 2011), as well as dental and skeletal fluorosis in children and adults (Maguire,

2014). In turn, this can lead to significant lower back pains (Namkaew and Wiwatanadate, 2012). It has been proposed that regularly consuming water with fluoride concentrations of at least 0.9 mg/l is the cause of at least 37% of dental fluorosis cases (McGrady *et al.*, 2012). Levy and Leclerc, (2012) also correlated fluoride in drinking water with bone diseases (Osteosarcoma) in adolescents and children. Sun *et al.*, (2013) discovered that cases of hypertension in adults could be linked to fluoride present in drinking water. They further emphasized that fluoride exposure could cause an increase in plasma Endothelin-1 (ET-1) levels. Liu *et al.*, (2014) also identified a link between fluoride exposure from drinking water and carotid artery atherosclerosis in adults. In a recent study conducted by Irigoyen–Camacho *et al.* (2016), reports showed that increased morbidity and mortality rate could be correlated with nutritional deficiencies propagated by fluoride intake. It should be noted that at low concentrations, ingesting fluoride from drinking water can hinder dental caries and some health authorities deliberately add fluoride to drinking water to reduce the incidence of enamel decay (Freire *et al.*, 2016).

In the urban regions of Nigeria, the wholesale provision of reliable access to drinking water has been made difficult due to increasing population and habitation spread within cities (Emenike *et al.*, 2016; Odjegba *et al.*, 2015, 2014), a similar case as seen in Tanzania. Many localities in southwestern Nigeria and Tanzania, in these regions, are supplied with surface water for their source of drinking water (Adekunle *et al.*, 2013). However, in many cases, these surface waters are heavily contaminated and polluted, particularly with respect to the microbial quality of the water, and are subsequently poorly treated making this water unfit for human consumption (John-Dewole, 2012; Tenebe *et al.*, 2017, 2016). For this reason, many people have accessed groundwater for their drinking water given its perceived higher quality (Adekunle *et al.*, 2013). However, given the noted pollution of such groundwater systems with fluoride and the evidenced

adverse effect on human health, a stronger link between fluoride concentration and its health impacts is needed to enable more thorough risk assessment and mitigation measures to be applied. Recently, researchers have adopted the human health risk assessment (HHRA) model to determine the adverse effect of absorbing or ingesting chemicals at a range of concentrations (Yang et al., 2012; Zhai et al., 2017). Therefore, this study seeks to consider two common pathways (ingestion and dermal) by which human populations can be exposed to high fluoride concentrations. In the same vein, the study capitalizes on the risk assessment indicators endorsed by the US EPA (2011) to assess the extent of fluoride contamination in groundwater and evaluate in detail, the health risk associated with fluoride pollution in groundwater. In furtherance of this, reports of elevated fluoride concentration in drinking water and its potential health risk has been investigated in Tunisia (Guissouma et al., 2017), Iran (Battaleb-Looie et al., 2013; Dehbandi et al., 2018; Yousefi et al., 2018), Ghana (Craig et al., 2015; Salifu et al., 2012), China (Zhang et al., 2017) and United Arab Emirates (Walia et al., 2017). But, to the best of our knowledge, there are a dearth of literatures in Nigeria with no previous investigation in the studied region in this regard. Therefore, this study focuses on the following objectives. First, to determine the spatial distribution of fluoride and other groundwater quality parameters in Abeokuta. Secondly, to analyze the interrelationship between fluoride and other water quality parameters. Thirdly, adopt geostatistical modeling in which semivariogram graphs will be used to describe and validate the extent of contamination via the interpolation of known concentration from sampled locations. Finally, assess the health risks associated with fluoride concentration in groundwater. To establish a more realistic base for judgement, ingestion and dermal pathways were investigated. Also, the receptors (individuals) were classified into seven age groups (6 – 12 months, 6 – 11 years, 11 – 16 years, 16 – 18 years, 18 – 21 years, ≥ 21 years and > 65 years). This will assist in adding relevant data to local rural

water management, policy and decision makers to take adequate measures in safeguarding the lives of residents in endemic fluoride regions.

2. Materials and Methods

Study area

Abeokuta, the capital of Ogun state, occupies 40.6 km² (latitude 7.17–7.25°N; longitudes 3.28–3.43°E). The population of Abeokuta is estimated to be 451,600 with an annual growth rate of 3.5% (National Population Commission, 2010). The area sits on a complex geological system, composed of a mix of rock from the Precambrian period. The complex spreads through the southwestern region of Nigeria, sharing a part with the Dahomey basin composed of sedimentary rock (Rahaman, 1976). The region is also linked to Lagos by river/canal (130 km) or by railway (77 km) and shares common borders with Ibadan, Shagamu, Ilaro, Ketuo, and Iseyin. The sample locations were targeted at regions with high population density.

“Fig. 1 is about here.”

Sample collection

The water samples analyzed in this study were obtained from taps that were connected directly to the underlying groundwater aquifer. In total, 63 water samples were collected from twenty-one locations (Fig. 1) in the study area (R1 – R21). The sampled taps were regularly used by householders mainly for consumption and domestic activities. At the point of collection, the taps were allowed to run for about 15 min before representative samples were collected to reflect the

status of the aquifer and the water consumed by the householder. Sample bottles (made of polyethylene) were washed with distilled water (mixed with 20% nitric acid) prior to sampling. The sample bottles were further rinsed three times with distilled water to remove any trace of acid and then air-dried before transporting to the sampling site. At the sampling location, the bottles were rinsed three times with tap water prior to collection to ensure no acid interference. After sample collection, the containers were sealed with screw corks, labeled appropriately, placed in a container filled with ice and immediately transferred to a refrigerator regulated at 4 °C.

As soon as each sample was collected, unstable and sensitive water quality parameters such as total dissolved solids (TDS), electrical conductivity (EC), temperature (Temp.), alkalinity (Alka.) and pH were measured in situ with a calibrated multiparameter probe (HANNA – HI2030 Salinity/TDS/EC meter and HANNA – HI98130). Standard analytical procedures (APHA, 2005) were followed to measure the ionic concentration of major ions. Sodium (Na^+), potassium (K^+), magnesium (Mg^{2+}), calcium (Ca^{2+}), iron (Fe^{2+}) and manganese (Mn) were measured using flame photometric method (Flame Atomic Absorption Spectrophotometry), dissolved silica (SiO_2) by molybdosilicate method with UV–Visible spectrometer and Nitrates (NO_3^-) concentration by UV–Visible spectrometer. Sulfate (SO_4^{2-}) concentration was determined by the turbidimetric method, bicarbonate (HCO_3^-), chloride (Cl^-), and carbonate (CO_3^{2-}) concentration were measured by volumetric method. A calibrated potentiometric ion-selection electrode (HANNA–HI5315) attached to a water-resistant portable ORP/pH/ISE meter (HANNA–HI98191) was used to measure the concentration of fluoride ion (F^-).

Quality control

Quality assurance was achieved through the implementation of standard laboratory procedures and quality control techniques which included standardized calibration, replication, use of analytical

grade reagent blanks and spikes, and following standard operating measures. Calibration of multiparameter instruments was performed after collecting samples from a location. The samples were analyzed in triplicate, and the mean value were recorded. During metal analysis, constant monitoring of reagent blanks was administered, and standard detection limits were maintained.

Geostatistical modeling

Water quality parameters were modelled spatially using the Empirical Bayesian Kriging (EBK) model. The EBK model automatically transforms the complicated aspects of the Kriging model by forming a restricted neighbor between a mapped property via interpolation. The interpolation relies on the subpopulation of the available dataset to produce independent trends (Samsonova et al., 2017). One essential element that differentiates the EBK model from other Kriging models is the ability to consider the uncertainties in semivariogram computation (Magesh et al., 2017). Thus, the operational module of the EBK estimation is based on the exploitation of original data to predict the semivariogram model (SVM) where a new set of data is generated at the original data point. Furthermore, the freshly simulated data is used to predict the SVM. During the estimation of the new SVM, predicted standard errors are processed at locations that had no observation, producing several spectrums of SVM due to repeated operations from original points. This study adopted the K-Bessel SVM which uses empirical transformations in simple remodeling. A study by Krivoruchko, (2011) noted that the method mentioned above is the most applicable, explicit and reliable technique but with a limitation of prolonged processing time.

2.1 Health risk assessment

Health risk assessment is a verified method that has been adopted extensively for the evaluation of potential hazards on human health after being exposed to certain chemicals over a period (US

EPA, 1989). In this study, the potential health risk of fluoride concentration on the population was evaluated. Due to the behavioral and physiological attributes of different age groups, the population was divided into seven age categories (6–12 months, 6–11 years, 11–16 years, 16–18 years, 18–21 years, ≥ 21 years and > 65 years) assessed from the US EPA exposure factor handbook (US EPA, 2011). Several pathways have been identified through which humans can be exposed to chemical risk. They include inhalation, dermal and ingestion pathways. However, this study considered dermal and ingestion pathways only because of the unavailability of the transfer efficiency of fluoride from water to air and its inhalation reference dose. Furthermore, inhalation was not considered as a major exposure route for fluoride (National Academy of Science, 2006). The chronic daily dose of fluoride via ingestion and dermal pathways were estimated using Eqn. (1) and Eqn. (2) based on (US EPA, 2011) recommendation.

$$CDD_{IN} = \frac{C_{fw} \times IR_w \times EF_r \times ED}{BW \times AT_r} \quad (1.1)$$

$$CDD_{DE} = \frac{C_{fw} \times SA \times K_p \times EF_r \times ED \times ET \times CF}{BW \times AT_r} \quad (1.2)$$

Where CDD_{IN} and CDD_{DE} are the estimated chronic daily dose of fluoride via ingestion and dermal exposure route respectively ($\mu g / kg \cdot day$); C_{fw} is the concentration of fluoride in drinking water ($\mu g / L$); IR_w is the ingestion rate (L / day); SA is the exposed skin area (cm^2); K_p is the dermal permeability coefficient for water (*unitless*); EF_r is the resident exposure frequency ($days / year$); ED is the exposure duration ($year$); ET is the water exposure time ($hours / day$); BW is body weight (kg); AT_r is the averaging resident time ($days / year$) and CF is the unit conversion factor (L / cm^3).

The hazard quotient (HQ) of fluoride exposure via ingestion and dermal pathways was calculated using Eqn. (3) and Eqn. (4)

$$HQ_{IN} = \frac{CDD_{IN}}{RfD} \quad (3)$$

$$HQ_{DE} = \frac{CDD_{DE}}{RfD} \quad (4)$$

Where HQ_{IN} and HQ_{DE} are the ingestion hazard quotient and dermal hazard quotient respectively; RfD is the reference dose of fluoride (equals 0.06 mg/kg-day according to the Integrated Risk Information System (IRIS) database of the US EPA) in a particular route. The reference values of each parameter used for calculating the CDD_{IN} , CDD_{DE} , HQ_{IN} and HQ_{DE} are compiled in Table S1 (in the supplementary material).

2.2 Data analysis

After the analyses of the water samples, the results were subject to descriptive statistical analyses. For each water quality parameter, the mean, minimum, maximum, and quartiles were calculated using GraphPad Prism 6 for Windows (GraphPad Software Inc.). The geospatial map of fluoride contamination and water quality parameters was achieved using ArcMap 10.3.1. The principal component analysis (influence plot, scree plot, score plot and loading plot) and correlation matrix were executed using Unscrambler X (CAMO software AS, version 10.4). The representation of the different water types on a Piper diagram was achieved using Rockworks17 64bit. The EBK model and semivariogram plots were calculated using geostatistical analyst tool in ArcMap 10.3.1.

3. Results and discussion

Within the study region, the TDS and EC values ranged from 498.33 to 2126.00 mg/L and 665.33 to 3314.67 $\mu\text{S}/\text{cm}$ respectively (Table S2). According to the results, 4.76% of the TDS samples were in a range considered desirable for drinking, 42.86% were in the permissible for drinking category and, 52.85% were useful for irrigation purposes as defined by WHO standards (WHO, 2011). Concerning EC, 23.80% were within the permissible limits for drinking, and the remaining 76.2% exceeded WHO stipulated standards. The cause of the increased TDS and EC concentrations could be due to heavy application of agro-chemicals, rainwater percolation, ion exchange and sediment dissolution (Chabukdhara et al., 2017). Relating the results of other water quality parameters with WHO guidance for drinking water (WHO, 2011), Cl^- values varied from 32.60 mg/L to 546.20 mg/L in all samples with 19% of samples exceeding the WHO threshold. The presence of chloride originates from dissolved chloride salts found in minerals as well as animal and human waste. Moreover, the heightened chloride concentration may be as a result of industrial and commercial activities within these zones.

Na^+ concentration varied from 55.97 mg/L to 514.73 mg/L. Out of the twenty-one locations sampled, only eight locations revealed Na^+ concentration exceeding the WHO threshold of 200 mg/L. It was evident that all locations had a high degree of variability in Na^+ and Cl^- concentrations with high standard deviation values of ± 112.88 and ± 140.88 respectively. It should be noted that Na^+ can be caused by cation exchange processes that occur in the aquifer. Furthermore, wastewater pollution from anthropogenic sources and intrusion from septic tanks may also increase sodium levels (Wayland et al., 2003).

HCO_3^- and CO_3^{2-} concentrations were observed in the range from 278.30 to 666.27 mg/L and 0–25.67 mg/L respectively. The concentration of HCO_3^- in the region exceeded WHO recommended

levels of 500 mg/L in 14.30% of the samples. Meanwhile, no permissible limit has been provided by the WHO standards for CO_3^{2-} in drinking water. Elevated levels of bicarbonate were likely to be from natural dissolution from rocks, as well as runoff, irrigation, and infiltration processes having contact with the groundwater systems during recharge (Rasool et al., 2016; Singh et al., 2013).

From the results displayed in Table S2, it was observed that SO_4^{2-} values varied from 35.73 mg/L to 978.60 mg/L. When the SO_4^{2-} values were compared with WHO guidelines for drinking water, 42.9% of the samples exceeded these limits. It is important to note here that elevated SO_4^{2-} concentrations in drinking water may result in respiratory illnesses (Subba Rao, 1993). NO_3^- concentrations ranged from 0.00 mg/L to 25.67 mg/L. These NO_3^- concentrations were low and within permissible limits, although its presence in water is attributed to anthropogenic activities resulting from fertilizer use (Tirkey et al., 2017).

Ca^{2+} and Mg^{2+} are important indicators of water hardness. Within the study area, Ca^{2+} values were within the permissible limits (200 mg/L) set by WHO except for sample point R17 (227.67 mg/L) that exceeded the limit. Some 33.33% of the water samples exceeded the WHO most desirable limits (75 mg/L) for Ca^{2+} while 52.38% of the analyzed water samples were above the WHO most desirable limit (50 mg/L) for Mg^{2+} concentration in drinking water. The reason for the variability of Mg^{2+} concentration may be associated with ion exchange linked with dissolved rock and soil minerals in the water. K^+ and Fe^{2+} values ranged from 2.07 to 9.30 mg/L and 0.02 to 2.96 mg/L respectively. All samples showed K^+ concentration lower than the WHO threshold but the Fe^{2+} concentration surpassed the WHO allowable limits in 38.10% of the samples. Although iron is not regarded as hazardous to human health, its presence could be seen as a nuisance or aesthetic pollutant. Fe^{2+} often coexists with Mn, which was found to be lower than the allowable limits

recommended by WHO guidelines for drinking water (WHO, 2011) in all samples. The co-existence of Mn and Fe^{2+} is proposed to occur from the natural dissolution from gneiss and biotite rock formation. Furthermore, a study by Magesh et al. (2017) showed that a deep groundwater aquifer could be laden with Fe^{2+} if ionic activities in aquifers were high.

The concentration of F^- ranged from 0.48 to 1.84 mg/L with a mean value of 1.23 mg/L. It was observed that 33% of the samples surpassed the WHO allowable limits for fluoride ion concentration in drinking water (1.5 mg/L). This result suggests that inhabitants may be faced with the risk of fluorosis, from consumption of this water. On the other hand, dental caries may be a risk when the fluoride content in drinking water falls below 0.5 mg/L. In line with this, it was also discovered that 14% of the samples had fluoride concentrations less than 0.5 mg/L, while 52.4% had fluoride concentration ranging from 0.5 to 1.5 mg/L which is the adequate dose for the development of healthy bones and teeth.

3.1 Water Quality Assessment

The hydrogeochemical facies of the region was characterized using Piper diagrams. The Piper plot consists of two triangles and a diamond-shaped diagram (Fig. 2a). The two triangles represent the plot of anion and cations, while the diamond-shaped plot shows the combination of the anion and cation fields. The concept of hydrogeochemical facies is derived from regions that contain identifiable characteristics of different anion and cation concentrations within the diamond-shape diagram.

From the Piper plot, it was observed that Na^+ and K^+ were the dominant cations. Nevertheless, Ca^{2+} and Mg^{2+} also contributed to the overall classification. In the anion region, HCO_3^- and SO_4^{2-} dominated the facies. With Na^+ dominating over other cations, it suggests the occurrence of ion

exchange activities as a result of rock weathering. However, the dominance of HCO_3^- and SO_4^{2-} also reveals ion contributions from silica weathering (Achary et al., 2016; Giridharan et al., 2009). In corroboration, Aghazadeh et al., (2016) and Barzegar et al., (2017) remarked that if the ratio of $\text{Ca}^+/\text{Mg}^{2+}$ ranges from 0.6 to any value greater than 2, it signifies the dissolution of dolomite and silicate rock materials in groundwater. After estimating the ratio of $\text{Ca}^+/\text{Mg}^{2+}$, the majority of the water samples (71.43%) produced ratios ranging from 0.65 to 5.24, indicating the interference of silicate and dolomitic constituents in the groundwater system. However, the general classification of all samples suggests 9% Ca–Mg–Cl– SO_4 , 24% Ca–Mg– HCO_3 , 29% Na–K–Cl– SO_4 , and 38% Na–K– HCO_3 water types.

3.2 Multivariate statistical investigation

Pearson's correlation analysis calculations have been deployed by different researchers in water quality evaluation to obtain the controlling ion in the hydrochemical process (P. C. Emenike et al., 2017; Giridharan et al., 2009; Li et al., 2013; Rasool et al., 2016). The data obtained from the CA served as a proportional measure to represent the association of one variable with the other. This study examined the interrelationships between the water quality parameters. In cases where the correlation coefficient (r) was less than 0.3, the relationship is regarded as a weak correlation. If r value ranges from 0.3 to 0.7, the relationship was considered moderate, and when the value of r was greater than 0.7 it is considered strong (Salifu et al., 2012; Xiao et al., 2015)

From the physico–chemical correlations (Table S3 in the supplementary material), fluoride was seen to have a strong positive relationship with TDS ($r = 0.79$), SO_4^{2-} ($r = 0.35$), EC ($r = 0.40$), and Mg^{2+} ($r = 0.34$). Similarly, fluoride showed a weak but positive relationship with Ca^{2+} ($r = 0.23$). Other relationships that can be drawn from the analysis show that there was a moderate positive correlation between pH and TDS ($r = 0.41$), EC ($r = 0.38$), Alka ($r = 0.46$), Fe^{2+} ($r =$

0.50) and Cl^- ($r = 0.34$). Similarly, a moderate negative relationship existed between $\text{pH} - \text{K}^+$ ($r = -0.45$) and $\text{pH} - \text{SiO}_2$ ($r = -0.50$).

In addition, the statistical analysis showed a strong positive inter-relationship between TDS – EC ($r = 0.91$), TDS – Mg^{2+} ($r = 0.78$), TDS – SO_4^{2-} ($r = 0.78$). Moderate positive inter-relationships exist between TDS – Ca^{2+} ($r = 0.44$), TDS – Na^+ ($r = 0.49$), TDS – HCO_3^- ($r = 0.66$) and TDS – Cl^- ($r = 0.59$). However, a moderate negative relationship existed between TDS – SiO_2 ($r = -0.56$).

The statistical study identified moderate positive correlations for EC – K^+ ($r = 0.34$), EC – Ca^{2+} ($r = 0.64$), EC – Mg^{2+} ($r = 0.57$), EC – Na^+ ($r = 0.34$), EC – HCO_3^- ($r = 0.65$), EC – Cl^- ($r = 0.54$) and a strong positive correlation for EC – SO_4^{2-} ($r = 0.79$). Other moderate positive relationships were seen in the results between $\text{Ca}^{2+} - \text{SO}_4^{2-}$ ($r = 0.66$), $\text{Mg}^{2+} - \text{SO}_4^{2-}$ ($r = 0.66$), $\text{SO}_4^{2-} - \text{HCO}_3^-$ ($r = 0.65$) while a strong positive relationship existed between $\text{Na}^+ - \text{Cl}^-$ ($r = 0.84$) and $\text{SO}_4^{2-} - \text{Cl}^-$ ($r = 0.76$).

In comparison, the average concentration of F^- obtained from this study were higher than the mean values obtained from the Birbhum district (Das and Nag, 2017), the Northern region of Ghana (Salifu et al., 2012), the Varahi river basin (Ravikumar and Somashekar, 2017) and less than that seen in the South of India (Viswanathan et al., 2009), Northern Tanzania (Shen and Schäfer, 2015), and Umarmkot sub-district, Pakistan (Rafique et al., 2015). It is important to note that the concentration of fluoride in water tends to increase when the TDS value is high (Rafique et al., 2009). Also looking at fluoride concentration with respect to pH, Guo *et al.*, (2012) noted that at pH 5.0 – 6.5, the solubility of fluoride is at its lowest. Saxena and Ahmed (2001) observed that the dissolution of fluoride occurs between pH 6 to pH 9. In this study, the pH of the water was 6.76, a condition where the solubility of fluoride was expected to be high. The presence of fluoride in water may be as a result of dissolution from quartzite and paleosols near the underlying

groundwater table (Amanambu and Egbinola, 2015; Chuah et al., 2016; Xiao et al., 2015) and it could be the reason for the moderate positive relationship existing between F^- and pH ($r = 0.53$). Also, in the correlation matrix (**Table S3** in the supplementary material), fluoride ions had a strong positive relationship with TDS ($r = 0.79$) and a moderate relationship with EC ($r = 0.40$), Mg^{2+} ($r = 0.34$), SO_4^{2-} ($r = 0.35$), and Alkalinity ($r = 0.40$). The moderate positive correlation between F^- and alkalinity confirms the penetration of fluoride enriched minerals from an alkaline environment into the groundwater systems.

3.3 Principal component analysis (PCA) of water parameters

PCA is a widely used technique that explains the variation in a large dataset where the variables are interconnected. It extracts information from the data by reducing dimensionality through variable reduction as well as qualitative structure–activity relationship. The interpretation of principal components (PC) can be linked to the hydrochemical characteristics of water samples. The loadings on each PC explains the water-rock interactions in the geochemical process (Fig. 2b). The most important parameters controlling the hydrochemical processes are mainly found in PC1, having the highest Eigenvalue. In this study, PCA was performed, and from the scree plot and explained variance (**Fig. 2c**), the PCA produced two components PC1 and PC2. PC1 contributed 90.09% of the total variance. Within the total variance explained by PC1, strong positive loadings were recorded in EC ($r = 0.9889$), TDS ($r = 0.9599$), SO_4^{2-} ($r = 0.8335$), HCO_3^- ($r = 0.6780$), Mg^{2+} ($r = 0.6597$), Ca^{2+} ($r = 0.5999$), Cl^- ($r = 0.6003$) and high negative loadings in SiO_2 ($r = -0.5243$). Considering the loadings mentioned above, PC1 can be regarded as a salinity index. PC2 explains 4.61% of the total variance with high negative loadings from Na^+ ($r = -0.7052$), Cl^- ($r = -0.6128$) and Mg^{2+} ($r = -0.4519$).

The positive loading of pH on PC1 suggests an interaction between silicate and carbonate materials. It also suggests dissolution processes involving gneiss and granite rock formations, which may be the reason for the dominance of Ca^{2+} , HCO_3^- and Mg^{2+} . These results support earlier works of Oke and Tijani (2012) and Ufoegbune et al. (2009), where it was observed that the geological formation of Abeokuta is mainly sedimentary and basement rocks of Paleozoic age enriched with MgO, SiO_2 , K_2O , and CaO. Concurrently, an increase in pH was seen when protons were consumed during the dissolution process. This may also be the reason why the pH had a positive loading on PC1. The varying pH values observed in these results is an indication that the groundwater system must have been recharged with water that passed through rock formations with a significant amount of salt.

Concerning the dominating parameters in PC1, the high positive loadings may be as a result of dissolved porphyritic biotite granite and porphyroblastic gneiss. This result supports the findings of Oke and Tijani, (2012) and confirms the presence of these rock formations contributing to the increase in TDS, EC, HCO_3^- , Mg^{2+} , Ca^{2+} , and Cl^- loadings recorded in PC1. The presence of these components represents a combined process comprising chemical weathering and mineralogical dissolution of rock constituents.

The score plot (Fig. 2d) accounts for the information and similarities within the samples analyzed and helps to understand the spatial distribution of the samples. From Fig. 2d, samples R14, R19, R12, R18, R13, and R21, were observed to have characteristics of similar water quality. Interestingly, within the samples, the total variance explained by PC1 (90.09%) received a high loading from R12 ($r = -737.455$), R13 ($r = -827.740$), R14 ($r = -1146.254$), R18 ($r = -705.517$), R21 ($r = -805.961$), R19 ($r = -962.665$) and R4 ($r = -1053.184$). Also from the results, the contribution from PC2 to the score plot emanates from R11 ($r = -697.740$). Similar contributions

can be seen from R6 and R7 with scores $r = -258.166$ and $r = -310.154$ respectively. The influence plot showing how the different samples contribute to the components is presented in Fig. 2 (e).

“Fig. 2(a–e) is about here.”

3.4 Geostatistical modeling

After analyzing the water quality parameters with the EBK model, the spatial distribution maps of all examined parameters are presented in Fig. 3(a–p). Four important factors revealed by the prediction statistics of the EBK model explained the authenticity of the model. They include, root mean squared predicted (RMSP), average standard error (ASE), mean standardized (MS), and root mean square standardized (RMSS) statistics. The results obtained established the potency of the different distribution of the EBK prediction model, one of which is associated with the closely related values of the ASE and RMSP values. From the results presented in Table 1, it could be seen that the ASE and RMSP are near, signifying the validity of the prediction. It is also important to note that RMSS should be close to 1 to explain the extent of estimation of the EBK model further. If the RMSS is > 1 , the prediction is said to be overestimated and if < 1 , the prediction is underestimated. Therefore, the results revealed the RMSS value of pH as 0.968; TDS, 0.967; EC, 0.966; F^- , 0.979; Fe^{2+} , 0.999; Mn, 0.998; Ca^{2+} , 0.966, K^+ , 0.993; Mg^{2+} , 0.970; Na^+ , 0.975; SO_4^{2-} , 0.910, SiO_2 , 0.981, HCO_3^- , 0.986; Cl^- , 0.972; NO_3^- , 0.959 and CO_3^{2-} , 0.986—authenticating the variability prediction since all values are close to 1. Furthermore, the MS value should be close to 0 for the prediction to be valid. This is confirmed, as the MS values in this study ranged from 0.072 to 0.092.

381 “Fig. 3 is about here.”

382 In the semivariograms of the examined water parameters (Fig 4a–4p), the blue crosses represent
383 the semivariance obtained from empirical transformation, the bold red lines represent the
384 intermediate distribution, the faint blue plots describe the different semivariograms distribution,
385 the faded red plots (dotted) displays the 25th and 75th percentile respectively, and the densely-
386 packed blue lines indicate the series of semivariogram passing through the zone. To examine the
387 stability of the model, the majority of the blue crosses should remain within the confines of the
388 faint blue spectrum (Magesh et al., 2017; Tenebe et al., 2018, 2017). This was the case observed
389 for all of the water parameters studied.

390 “Fig. 4 is about here.”

391 3.5 Fluoride risk assessment

392 Ingestion risk

393 The hazard quotient (HQ) associated with fluoride concentration on different age classification (6–
394 12 months, 6–11 years, 11–16 years, 16–18 years, 18–21 years, ≥ 21 years and > 65 years) was
395 evaluated, integrating the indicators obtained from the US EPA Exposure Factor Handbook (US
396 EPA, 2011) as well as the fluoride concentration in the groundwater from the sampled locations.
397 The non-carcinogenic risks were computed, and the age classification with high values of HQ_{IN}
398 are presented in Table 2 and Table S4 (in the supplementary material). The mean CDD_{IN} values
399 ranged from 53.846–201.832 $\mu\text{g}/(\text{kg day})$ for age 6–12 months. The mean CDD_{IN} values for age 6
400 – 11 years varied from 22.075 to 82.744 $\mu\text{g}/(\text{kg day})$. The mean CDD_{IN} values for age 11–16 years
401 varied from 16.454 to 61.674 $\mu\text{g}/(\text{kg day})$. Similarly, the mean CDDs for age classifications 16–
402 18 years, 18–21 years, ≥ 21 years and > 65 years varied from 12.902 to 48.362 $\mu\text{g}/(\text{kg day})$, 16.962

to 63.577 $\mu\text{g}/(\text{kg day})$, 18.282 to 68.525 $\mu\text{g}/(\text{kg day})$ and 16.721 to 62.672 $\mu\text{g}/(\text{kg day})$ respectively, in relation to water ingestion (Table S4 in the supplementary material). After computing the HQ_{IN} , further observation revealed that 90.5% of the sampled locations were above the permissible level because for age classification 6–12 months, because the HQ_{IN} values were greater than 1. The implication is that the children in the 6 – 12 months age range are more likely to suffer from health complications associated with consumption of water laden with a high concentration of fluoride (Ding et al., 2011). Also, children within the age range of 6 – 11 years were also expected to be affected as 42.9% of the sampled region exceeded the HQ_{IN} limits.

Furthermore, 4.8% of the modelled exposures surpassed the acceptable HQ_{IN} limit for age classes 11–16 years and > 65 years, 9.5% of the sampled region exceeded the permissible HQ_{IN} level for age 18–21 years, 19.05% of the study location was beyond the allowable HQ_{IN} limits for age ≥ 21 years. No risk was modelled for age class 16 – 18 years in the region. Despite the fact that age classifications 11–16 years, 18–21 years, ≥ 21 years and > 65 years had overall low percentage risks, it was observed that at specific locations (R16 and R17), much higher risks were seen across all age classifications noted above. This identifies explicitly the need for more extensive water treatment at locations R16 and R17 since the region is prone to high fluoride concentrations in the tap water.

Dermal risk

Table S5 (in the supplementary material) and Table 3 shows the dermal CDD_{DE} and HQ_{DE} values respectively. The dermal mean CDD_{DE} varied from 0.125 $\mu\text{g}/(\text{kg day})$ to 0.470 $\mu\text{g}/(\text{kg day})$ and 0.111 $\mu\text{g}/(\text{kg day})$ to 0.418 $\mu\text{g}/(\text{kg day})$ for age classification 6–12 months and 6–11 years

respectively. Correspondingly, the CDD_{DE} for age class 11–16years and 16–18years varied from 0.073 $\mu\text{g}/(\text{kg day})$ to 0.275 $\mu\text{g}/(\text{kg day})$ and 0.068 $\mu\text{g}/(\text{kg day})$ to 0.253 $\mu\text{g}/(\text{kg day})$. After computing the chronic daily dose as a result of dermal exposure (CDD_{DE}) for age class 18–21years, ≥ 21 years and > 65 years, the values ranged from 0.096 $\mu\text{g}/(\text{kg day})$ to 0.362 $\mu\text{g}/(\text{kg day})$, 0.083 $\mu\text{g}/(\text{kg day})$ to 0.310 $\mu\text{g}/(\text{kg day})$ and 0.081 $\mu\text{g}/(\text{kg day})$ to 0.303 $\mu\text{g}/(\text{kg day})$ respectively. The HQ_{DE} obtained in this study suggests low risk via dermal exposure for all age classification ($HQ_{DE} - 1$). However, the HQ_{DE} values presented in the results establish the need for attention, especially now that the aftermath of climate change poses significant change to groundwater resources. Significant health impediments, in addition to dental and skeletal fluorosis, such as neurotoxicological diseases (Choi et al., 2012), skeletal cancer (Bassin et al., 2006), hypertension (Sun et al., 2013), carotid artery atherosclerosis (Liu et al., 2014) and cardiac dysfunction (Varol et al., 2010) or possibly death may occur due to long-term exposure of fluoride. In other words, if the current trend of fluoride contamination occurs continuously in the study area, the devastating effect on lives will be enormous since survival possibilities rely on the availability of clean (non-contaminated) drinking water (Emenike et al., 2017).

4. Conclusion

The different ionic concentration of groundwater, fluoride concentration and its associated health risk were investigated in Abeokuta, Nigeria. Considering the water quality of the sixty-three taps analyzed, only about 5% were found to be fit for consumption (based on the percentage violation of TDS from WHO standards). According to the WHO guidelines for drinking water quality (WHO, 2011), parameters such as TDS, EC, F^- and SO_4^{2-} exceeded allowable limits. The findings in this study revealed that chemical weathering and dissolved rock compounds were responsible for the presence of F^- , HCO_3^- , Mg^{2+} , high TDS and EC in the groundwater. The CA and PCA

techniques validate the interrelationship of elements and its potential source as it reveals a statistical relationship between F^- and TDS, EC, Alkalinity, Mg^{2+} , and SO_4^{2-} . The classification of the water types could be ranked as Na–K– HCO_3^- –Na–K–Cl– SO_4 –Ca–Mg– HCO_3^- –Ca–Mg–Cl– SO_4 type. The information obtained from the EBK model validates the prediction of the spatial distribution as the standardized RMS values were close to 1. Also, the values of ASE and RMSP were almost equal which validates the authenticity of the spatial model. Further observation revealed that 90.5% of the modelled exposure was above the standard level for age classification 6–12 months. 4.8% of the modelled exposures exceeded the acceptable HQ_{IN} limit for age classes 11–16 years and > 65 years, 9.5% of the sampled region exceeded the permissible HQ_{IN} level for age 18–21 years and 19.05% of the study location was beyond the allowable HQ_{IN} limits for age \geq 21 years.

Acknowledgement

The authors wish to thank the management of Covenant University for the enabling atmosphere for the research. We want to also appreciate the advice given by Dr. Jitka MacAdam (Cranfield Water Science Institute. School of Water, Energy and Environment, Cranfield University, United Kingdom). Also, we wish to thank the anonymous reviewers for their technical contributions required to bring this paper to this state.

References

- Achary, M.S., Panigrahi, S., Satpathy, K.K., Prabhu, R.K., Panigrahy, R.C., 2016. Health risk assessment and seasonal distribution of dissolved trace metals in surface waters of Kalpakkam, southwest coast of Bay of Bengal. *Reg. Stud. Mar. Sci.* 6, 96–108. <https://doi.org/10.1016/j.rsma.2016.03.017>
- Adekunle, A.A., Adedayo O. Badejo, Abiola O. Oyerinde, 2013. Pollution Studies on Ground Water Contamination : Water Quality of Abeokuta , Ogun State , South West Nigeria. *J. Environ. Earth Sci.* 3, 161–166.
- Aghazadeh, N., Chitsazan, M., Golestan, Y., 2016. Hydrochemistry and quality assessment of groundwater in the Ardabil area , Iran. *Appl. Water Sci.* 7, 3599–3616. <https://doi.org/10.1007/s13201-016-0498-9>
- Amanambu, A.C., Egbinola, C.N., 2015. Geogenic contamination of groundwater in shallow aquifers in Ibadan, south-west Nigeria. *Manag. Environ. Qual. An Int. J.* 26, 327–341. <https://doi.org/10.1108/MEQ-12-2013-0135>
- Amini, M., Abbaspour, K.C., Berg, M., Winkel, L., Hug, S.J., Hoehn, E., Yang, H., Johnson, C.A., 2008. Statistical modeling of global geogenic arsenic contamination in groundwater. *Env. Sci Technol* 42, 3669–3675.
- Barzegar, R., Asghari Moghaddam, A., Tziritis, E., 2017. Hydrogeochemical features of groundwater resources in Tabriz plain, northwest of Iran. *Appl. Water Sci.* <https://doi.org/10.1007/s13201-017-0550-4>
- Bassin, E.B., Wypij, D., Davis, R.B., Mittleman, M.A., 2006. Age-specific fluoride exposure in drinking water and osteosarcoma (United States). *Cancer Causes Control* 17, 421–428. <https://doi.org/10.1007/s10552-005-0500-6>
- Battaleb-Looie, S., Moore, F., Malde, M.K., Jacks, G., 2013. Fluoride in groundwater, dates and wheat: Estimated exposure dose in the population of Bushehr, Iran. *J. Food Compos. Anal.* 29, 94–99. <https://doi.org/10.1016/j.jfca.2012.08.001>
- Bhatnagar, A., Kumar, E., Sillanpää, M., 2011. Fluoride removal from water by adsorption-A review. *Chem. Eng. J.* 171, 811–840. <https://doi.org/10.1016/j.cej.2011.05.028>
- Chabukdhara, M., Gupta, S.K., Kotecha, Y., Nema, A.K., 2017. Groundwater quality in Ghaziabad district, Uttar Pradesh, India: Multivariate and health risk assessment. *Chemosphere* 179, 167–178. <https://doi.org/10.1016/j.chemosphere.2017.03.086>
- Choi, A.L., Sun, G., Zhang, Y., Grandjean, P., 2012. Developmental Fluoride Neurotoxicity: A Systematic Review and Meta-Analysis. *Environ. Health Perspect.* 1362, 1362–1368.
- Chuah, C.J., Lye, H.R., Ziegler, A.D., Wood, S.H., Kongpun, C., Rajchagool, S., 2016. Fluoride: A naturally-occurring health hazard in drinking-water resources of Northern Thailand. *Sci. Total Environ.* 545–546, 266–279. <https://doi.org/10.1016/j.scitotenv.2015.12.069>
- Craig, L., Lutz, A., Berry, K.A., Yang, W., 2015. Recommendations for fluoride limits in drinking water based on estimated daily fluoride intake in the Upper East Region, Ghana. *Sci. Total*

Environ. 532, 127–137. <https://doi.org/10.1016/j.scitotenv.2015.05.126>

Das, S., Nag, S.K., 2017. Application of multivariate statistical analysis concepts for assessment of hydrogeochemistry of groundwater—a study in Suri I and II blocks of Birbhum District, West Bengal, India. *Appl. Water Sci.* 7, 873–888. <https://doi.org/10.1007/s13201-015-0299-6>

Dehbandi, R., Moore, F., Keshavarzi, B., 2018. Geochemical sources, hydrogeochemical behavior, and health risk assessment of fluoride in an endemic fluorosis area, central Iran. *Chemosphere* 193, 763–776. <https://doi.org/10.1016/j.chemosphere.2017.11.021>

Ding, Y., YanhuiGao, Sun, H., Han, H., Wang, W., Ji, X., Liu, X., Sun, D., 2011. The relationships between low levels of urine fluoride on children’s intelligence, dental fluorosis in endemic fluorosis areas in Hulunbuir, Inner Mongolia, China. *J. Hazard. Mater.* 186, 1942–1946. <https://doi.org/10.1016/j.jhazmat.2010.12.097>

Emenike, C.P., Tenebe, I.T., Omole, D.O., Ngene, B.U., Oniemayin, B.I., Maxwell, O., Onoka, B.I., 2017. Accessing safe drinking water in sub-Saharan Africa: Issues and challenges in South-West Nigeria. *Sustain. Cities Soc.* 30, 263–272. <https://doi.org/10.1016/j.scs.2017.01.005>

Emenike, P.C., Omole, D.O., Ngene, B.U., Tenebe, I.T., 2016. Potentiality of agricultural adsorbent for the sequestering of metal ions from wastewater. *Glob. J. Environ. Sci. Manag.* 2, 411–442. <https://doi.org/10.22034/gjesm.2016.02.04.010>

Emenike, P.C., Tenebe, T.I., Omeje, M., Osinubi, D.S., 2017. Health risk assessment of heavy metal variability in sachet water sold in Ado-Odo Ota, South-Western Nigeria. *Environ. Monit. Assess.* 189, 1–16. <https://doi.org/10.1007/s10661-017-6180-3>

EPA, 2010. Fluoride: Exposure and Relative Source Contribution Analysis. Washington, D.C.

Fawell, J., Bailey, K., Chilton, J., Dahi, E., Fewtrell, L., Magara, Y., 2006. Fluoride in Drinking-water, World Health Organization. <https://doi.org/10.1007/BF01783490>

Freire, I.R., Pessan, J.P., Amaral, J.G., Martinhon, C.C.R., Cunha, R.F., Delbem, A.C.B., 2016. Anticaries effect of low-fluoride dentifrices with phosphates in children: A randomized, controlled trial. *J. Dent.* 50, 37–42. <https://doi.org/10.1016/j.jdent.2016.04.013>

Giridharan, L., Venugopal, T., Jayaprakash, M., 2009. Assessment of water quality using chemometric tools: A case study of river cooum, South India. *Arch. Environ. Contam. Toxicol.* 56, 654–669. <https://doi.org/10.1007/s00244-009-9310-2>

Guissouma, W., Hakami, O., Al-Rajab, A.J., Tarhouni, J., 2017. Risk assessment of fluoride exposure in drinking water of Tunisia. *Chemosphere* 177, 102–108. <https://doi.org/10.1016/j.chemosphere.2017.03.011>

Guo, H., Zhang, Y., Xing, L., Jia, Y., 2012. Spatial variation in arsenic and fluoride concentrations of shallow groundwater from the town of Shapai in the Hetao basin, Inner Mongolia. *Appl. Geochemistry* 27, 2187–2196. <https://doi.org/10.1016/j.apgeochem.2012.01.016>

Irigoyen-Camacho, M.E., García Pérez, A., Mejía González, A., Huizar Alvarez, R., 2016. Nutritional status and dental fluorosis among schoolchildren in communities with different

542 drinking water fluoride concentrations in a central region in Mexico. *Sci. Total Environ.* 541,
543 512–519. <https://doi.org/10.1016/j.scitotenv.2015.09.085>

544 Izquierdo-Vega, J.A., Sánchez-Gutiérrez, M., Del Razo, L.M., 2008. Decreased in vitro fertility in
545 male rats exposed to fluoride-induced oxidative stress damage and mitochondrial
546 transmembrane potential loss. *Toxicol. Appl. Pharmacol.* 230, 352–357.
547 <https://doi.org/10.1016/j.taap.2008.03.008>

548 Jha, S.K., Mishra, V.K., Sharma, D.K., Damodaran, T., 2011. Fluoride in the environment and its
549 metabolism in humans. *Rev. Environ. Contam. Toxicol.* 211, 121–142.
550 https://doi.org/10.1007/978-1-4419-8011-3_4

551 John-Dewole, O., 2012. Adverse Effects of Inadequate Water Supply on Human Health : a case
552 study of Kajola Local Government in Oyo State , Nigeria By. *Greener J. Med. Sci.* 2, 115–
553 119.

554 Kaoud, H., Kalifa, B., 2010. Effect of fluoride, cadmium and arsenic intoxication on brain and
555 learning–memory ability in rats. *Toxicol. Lett.* 196, S53.
556 <https://doi.org/10.1016/j.toxlet.2010.03.212>

557 Krivoruchko, K., 2011. Spatial Statistical Data Analysis for GIS Users Spatial Statistical Data
558 Analysis for GIS Users, Esri Press, Rehlands, CA. Esri Press, Rehlands, CA.

559 Levy, M., Leclerc, B.S., 2012. Fluoride in drinking water and osteosarcoma incidence rates in the
560 continental United States among children and adolescents. *Cancer Epidemiol.* 36, 83–88.
561 <https://doi.org/10.1016/j.canep.2011.11.008>

562 Li, P., Qian, H., Wu, J., Zhang, Y., Zhang, H., 2013. Major Ion Chemistry of Shallow Groundwater
563 in the Dongsheng Coalfield, Ordos Basin, China. *Mine Water Environ.* 32, 195–206.
564 <https://doi.org/10.1007/s10230-013-0234-8>

565 Liu, H., Gao, Y., Sun, L., Li, M., Li, B., Sun, D., 2014. Assessment of relationship on excess
566 fluoride intake from drinking water and carotid atherosclerosis development in adults in
567 fluoride endemic areas, China. *Int. J. Hyg. Environ. Health* 217, 413–420.
568 <https://doi.org/10.1016/j.ijheh.2013.08.001>

569 Magesh, N.S., Chandrasekar, N., Elango, L., 2017. Trace element concentrations in the
570 groundwater of the Tamiraparani river basin, South India: Insights from human health risk
571 and multivariate statistical techniques. *Chemosphere* 185, 468–479.
572 <https://doi.org/10.1016/j.chemosphere.2017.07.044>

573 Maguire, A., 2014. ADA clinical recommendations on topical fluoride for caries prevention. *Evid.*
574 *Based. Dent.* <https://doi.org/10.1038/sj.ebd.6401019>

575 McGrady, M.G., Ellwood, R.P., Srisilapanan, P., Korwanich, N., Worthington, H. V., Pretty, I.A.,
576 2012. Dental fluorosis in populations from Chiang Mai, Thailand with different fluoride
577 exposures - Paper 1: assessing fluorosis risk, predictors of fluorosis and the potential role of
578 food preparation. *BMC Oral Health* 12, 1. <https://doi.org/10.1186/1472-6831-12-16>

579 Namkaew, M., Wiwatanadate, P., 2012. Association of fluoride in water for consumption and
580 chronic pain of body parts in residents of San Kamphaeng district, Chiang Mai, Thailand.
581 *Trop. Med. Int. Heal.* 17, 1171–1176. <https://doi.org/10.1111/j.1365-3156.2012.03061.x>

582 National Academy of Science, 2006. Fluoride in Drinking Water: A Scientific Review of EPA's
583 Standards. The National Academies Press. Washington, D.C. <https://doi.org/10.17226/11571>

584 National Population Commission, 2010. Population Distribution by Sex, State, LGA & Senatorial
585 District, 2006 Population and Housing Census.

586 Odjegba, E., Idowu, O., Ikenweiwe, N., Martins, O., Sadeeq, A., 2015. Public Perception of
587 Potable Water Supply in Abeokuta. *J. Appl. Sci. Environ. Manag.* 19, 5–9.

588 Odjegba, E.E., Idowu, O.A., Oluwasanya, G.O., Ikenweiwe, N.B., Martins, O., 2014. Assessment
589 of Water Demand and Seasonal Variation of Bacteriological Content of Public Water Systems
590 in Abeokuta ... *Int. J. Inst. Ecol. Environ. Stud.* 2, 81–92.

591 Oke, S.A., Tijani, M.N., 2012. Impact of chemical weathering on groundwater chemistry of
592 Abeokuta area. *J. Elixir Pollut.* 46, 8498–8503.

593 Rafique, T., Naseem, S., Ozsvath, D., Hussain, R., Bhanger, M.I., Usmani, T.H., 2015.
594 Geochemical controls of high fluoride groundwater in Umarkot Sub-District, Thar Desert,
595 Pakistan. *Sci. Total Environ.* 530–531, 271–278.
596 <https://doi.org/10.1016/j.scitotenv.2015.05.038>

597 Rafique, T., Naseem, S., Usmani, T.H., Bashir, E., Khan, F.A., Bhanger, M.I., 2009. Geochemical
598 factors controlling the occurrence of high fluoride groundwater in the Nagar Parkar area,
599 Sindh, Pakistan. *J. Hazard. Mater.* 171, 424–430.
600 <https://doi.org/10.1016/j.jhazmat.2009.06.018>

601 Rahaman, M., 1976. Review of the basement geology of South-Western Nigeria. In: C.A. Kogbe
602 (Ed.) *Geology of Nigeria*. Elizabethan Publishing Co., Lagos, Nigeria.

603 Rasool, A., Xiao, T., Farooqi, A., Shafeeque, M., Masood, S., Ali, S., Fahad, S., Nasim, W., 2016.
604 Arsenic and heavy metal contaminations in the tube well water of Punjab, Pakistan and risk
605 assessment: A case study. *Ecol. Eng.* 95, 90–100.
606 <https://doi.org/10.1016/j.ecoleng.2016.06.034>

607 Ravikumar, P., Somashekar, R.K., 2017. Principal component analysis and hydrochemical facies
608 characterization to evaluate groundwater quality in Varahi river basin, Karnataka state, India.
609 *Appl. Water Sci.* 7, 745–755. <https://doi.org/10.1007/s13201-015-0287-x>

610 Salifu, A., Petrusevski, B., Ghebremichael, K., Buamah, R., Amy, G., 2012. Multivariate statistical
611 analysis for fluoride occurrence in groundwater in the Northern region of Ghana. *J. Contam.*
612 *Hydrol.* 140–141, 34–44. <https://doi.org/10.1016/j.jconhyd.2012.08.002>

613 Samsonova, V.P., Blagoveshchenskii, Y.N., Meshalkina, Y.L., 2017. Use of empirical Bayesian
614 kriging for revealing heterogeneities in the distribution of organic carbon on agricultural
615 lands. *Eurasian Soil Sci.* 50, 305–311. <https://doi.org/10.1134/S1064229317030103>

616 Saxena, V.K., Ahmed, S., 2001. Dissolution of fluoride in groundwater: A water-rock interaction
617 study. *Environ. Geol.* 40, 1084–1087. <https://doi.org/10.1007/s002540100290>

618 Shen, J., Schäfer, A.I., 2015. Factors affecting fluoride and natural organic matter (NOM) removal
619 from natural waters in Tanzania by nanofiltration/reverse osmosis. *Sci. Total Environ.* 527–
620 528, 520–529. <https://doi.org/10.1016/j.scitotenv.2015.04.037>

Shivaprakash, P.K., Ohri, K., Noorani, H., 2011. Relation between dental fluorosis and intelligence quotient in school children of Bagalkot district. *J. Indian Soc. Pedod. Prev. Dent.* 29, 117–120. <https://doi.org/10.4103/0970-4388.84683>

Singh, C.K., Kumari, R., Singh, N., Mallick, J., Mukherjee, S., 2013. Fluoride enrichment in aquifers of the Thar desert: Controlling factors and its geochemical modelling. *Hydrol. Process.* 27, 2462–2474. <https://doi.org/10.1002/hyp.9247>

Singh, C.K., Mukherjee, S., 2015. Aqueous geochemistry of fluoride enriched groundwater in arid part of Western India. *Environ. Sci. Pollut. Res.* 22, 2668–2678. <https://doi.org/10.1007/s11356-014-3504-5>

Smedley, P., Nkotagu, H., Pelig-Ba, K., MacDonald, A., Tyler-Whittle, R., Whitehead, E., Kinniburgh, D., 2002. Fluoride in groundwater from high-fluoride areas in Ghana and Tanzania. “Minimising fluoride in drinking water in problem aquifers.” *Br. Geol. Surv. Comm. Report*, CR/02/316 77.

Subba Rao, N., 1993. Environmental impact of industrial effluents in groundwater regions of Visakhapatnam Industrial Complex. *Indian J. Geol.* 65, 35–43.

Subba Rao, N., Subrahmanyam, A., Babu Rao, G., 2013. Fluoride-bearing groundwater in Gummanampadu Sub-basin, Guntur District, Andhra Pradesh, India. *Environ. Earth Sci.* 70, 575–586. <https://doi.org/10.1007/s12665-012-2142-9>

Sun, L., Gao, Y., Liu, H., Zhang, W., Ding, Y., Li, B., Li, M., Sun, D., 2013. An assessment of the relationship between excess fluoride intake from drinking water and essential hypertension in adults residing in fluoride endemic areas. *Sci. Total Environ.* 443, 864–869. <https://doi.org/10.1016/j.scitotenv.2012.11.021>

Tenebe, I.T., Emenike, C.P., Ogbiye, A.S., Ngene, B.U., Omeje, M., Olatunji, O.O., 2018. A laboratory assessment of the effect of varying roughness on dissolved oxygen using error correction method. *Cogent Eng.* 0, 1–11. <https://doi.org/10.1080/23311916.2018.1427191>

Tenebe, I.T., Ogbiye, A., Omole, D.O., Emenike, P.C., 2016. Estimation of longitudinal dispersion co-efficient: A review. *Cogent Eng.* 3. <https://doi.org/10.1080/23311916.2016.1216244>

Tenebe, I.T., Ogbiye, A.S., Omole, D.O., Emenike, P.C., 2017. Modelling and sensitivity analysis of varying roughness effect on dispersion coefficient: a laboratory study 21298, 1–7. <https://doi.org/10.5004/dwt.2017.21298>

Tirkey, P., Bhattacharya, T., Chakraborty, S., Baraik, S., 2017. Assessment of groundwater quality and associated health risks: A case study of Ranchi city, Jharkhand, India. *Groundw. Sustain. Dev.* 5, 85–100. <https://doi.org/10.1016/j.gsd.2017.05.002>

Ufoegbune, G., Lamidi, K., Awomeso, J., Eruola, A., Idowu, O., 2009. Hydro-geological characteristics and groundwater quality assessment in some selected communities of Abeokuta, Southwest Nigeria. *J. Environ. Chem. Ecotoxicol.* 1, 010–022.

US EPA, 2011. Exposure Factors Handbook: 2011 Edition, 2011 Editi. ed, U.S. Environmental Protection Agency. <https://doi.org/EPA/600/R-090/052F>

US EPA, 1989. Risk Assessment Guidance for Superfund Volume I Human Health Evaluation

Manual (Part A), US EPA. <https://doi.org/EPA/540/1-89/002>

- Varol, E., Akcay, S., Ersoy, I.H., Ozaydin, M., Koroglu, B.K., Varol, S., 2010. Aortic elasticity is impaired in patients with endemic fluorosis. *Biol. Trace Elem. Res.* 133, 121–127. <https://doi.org/10.1007/s12011-009-8578-4>
- Viswanathan, G., Jaswanth, A., Gopalakrishnan, S., Siva ilango, S., Aditya, G., 2009. Determining the optimal fluoride concentration in drinking water for fluoride endemic regions in South India. *Sci. Total Environ.* 407, 5298–5307. <https://doi.org/10.1016/j.scitotenv.2009.06.028>
- Walia, T., Abu Fanas, S., Akbar, M., Eddin, J., Adnan, M., 2017. Estimation of fluoride concentration in drinking water and common beverages in United Arab Emirates (UAE). *Saudi Dent. J.* 29, 117–122. <https://doi.org/10.1016/j.sdentj.2017.04.002>
- Wayland, K.G., Long, D.T., Hyndman, D.W., Pijanowski, B.C., Woodhams, S.M., Haack, S.K., 2003. with Synoptic Sampling and R-Mode Factor Analysis. *J. Environ. Qual.* 32, 180–190.
- WHO, 2011. WHO Guidelines for Drinking-water Quality., 4th Editio. ed, World Health Organization. [https://doi.org/10.1016/S1462-0758\(00\)00006-6](https://doi.org/10.1016/S1462-0758(00)00006-6)
- Xiao, J., Jin, Z., Zhang, F., 2015. Geochemical controls on fluoride concentrations in natural waters from the middle Loess Plateau, China. *J. Geochemical Explor.* 159, 252–261. <https://doi.org/10.1016/j.gexplo.2015.09.018>
- Yang, M., Fei, Y., Ju, Y., Ma, Z., Li, H., 2012. Health risk assessment of groundwater pollution- A case study of typical city in North China plain. *J. Earth Sci.* 23, 335–348. <https://doi.org/10.1007/s12583-012-0260-7>
- Yousefi, M., Ghoochani, M., Hossein Mahvi, A., 2018. Health risk assessment to fluoride in drinking water of rural residents living in the Poldasht city, Northwest of Iran. *Ecotoxicol. Environ. Saf.* 148, 426–430. <https://doi.org/10.1016/j.ecoenv.2017.10.057>
- Zhai, Y., Zhao, X., Teng, Y., Li, X., Zhang, J., Wu, J., Zuo, R., 2017. Groundwater nitrate pollution and human health risk assessment by using HHRA model in an agricultural area, NE China. *Ecotoxicol. Environ. Saf.* 137, 130–142. <https://doi.org/10.1016/j.ecoenv.2016.11.010>
- Zhang, L., Huang, D., Yang, J., Wei, X., Qin, J., Ou, S., Zhang, Z., Zou, Y., 2017. Probabilistic risk assessment of Chinese residents' exposure to fluoride in improved drinking water in endemic fluorosis areas. *Environ. Pollut.* 222, 118–125. <https://doi.org/10.1016/j.envpol.2016.12.074>

Table 1: Prediction error information obtained from the empirical Bayesian kriging (EBK) model

	pH	TDS	EC	F ⁻	Fe ²⁺	Mn	Ca ²⁺	K ⁺	Mg ²⁺	Na ⁺	SO ₄ ²⁻	SiO ₂	HCO ₃ ⁻	Cl ⁻	NO ₃ ⁻	CO ₃ ²⁻
Mean	0.104	0.832	12.048	0.004	0.007	0.002	0.746	0.086	-4.519	1.348	3.378	-0.162	3.550	3.727	0.111	0.229
RMS Pred.	0.391	451.368	679.930	0.406	0.707	0.023	40.291	2.114	85.810	104.470	192.912	2.009	110.187	135.657	1.859	7.985
MS	0.022	0.005	0.022	0.009	0.019	0.092	0.017	0.041	-0.054	0.009	0.015	-0.072	0.030	0.021	0.555	0.029
RMSS	0.968	0.967	0.966	0.979	0.999	0.998	0.966	0.993	0.970	0.975	0.910	0.981	0.986	0.972	0.959	0.968
ASE	0.402	464.203	716.913	0.416	0.697	0.023	41.830	2.128	88.373	107.705	215.608	2.037	109.195	141.679	1.970	8.276

Table 2: Hazard quotients via ingestion pathway (**HQ_{IN}**) for different age classification

REGION	HQ _{IN} VALUES						
	(6 – 12months)	(6 – 11years)	(11 – 16years)	(16 – 18years)	(18 – 21years)	(≥ 21years)	(> 65years)
R1	*1.877	0.770	0.574	0.450	0.591	0.637	0.583
R2	*2.405	**0.986	0.735	0.576	0.758	0.817	0.747
R3	*2.833	*1.161	0.866	0.679	0.892	**0.962	0.880
R4	*3.016	*1.236	0.922	0.723	**0.950	*1.024	0.937
R5	*2.021	0.828	0.617	0.484	0.637	0.686	0.628
R6	*2.906	*1.191	0.888	0.696	0.915	*0.987	0.902
R7	*2.369	**0.971	0.724	0.568	0.746	0.804	0.736
R8	*1.215	0.498	0.371	0.291	0.383	0.412	0.377
R9	0.913	0.374	0.279	0.219	0.288	0.310	0.283
R10	*2.650	*1.086	0.810	0.635	0.835	0.900	0.823
R11	*1.484	0.608	0.453	0.355	0.467	0.504	0.461
R12	0.910	0.373	0.278	0.218	0.287	0.309	0.282
R13	*2.473	*1.014	0.756	0.592	0.779	0.839	0.768
R14	*2.259	0.926	0.690	0.541	0.712	0.767	0.701
R15	*3.034	*1.244	0.927	0.727	**0.956	*1.030	0.942
R16	*3.364	*1.379	*1.028	0.806	*1.060	*1.142	*1.045
R17	*3.217	*1.319	**0.983	0.771	*1.013	*1.092	**0.999
R18	*2.430	**0.996	0.742	0.582	0.765	0.825	0.755
R19	*2.295	0.941	0.701	0.550	0.723	0.779	0.713
R20	*2.814	*1.154	0.860	0.674	0.887	**0.956	0.874
R21	0.897	0.368	0.274	0.215	0.283	0.305	0.279

* HQ values exceeding the US EPA and WHO standards

** HQ values exceeding 0.95

Table 3: Hazard quotients via dermal pathway (**HQ_{DE}**) for different age classification

REGION	HQ_{DE} VALUES						
	(6–12months)	(6–11years)	(11–16years)	(16–18years)	(18–21years)	(≥ 21years)	(> 65years)
R1	0.004	0.004	0.003	0.002	0.003	0.003	0.003
R2	0.006	0.005	0.003	0.003	0.004	0.004	0.004
R3	0.007	0.006	0.004	0.004	0.005	0.004	0.004
R4	0.007	0.006	0.004	0.004	0.005	0.005	0.005
R5	0.005	0.004	0.003	0.003	0.004	0.003	0.003
R6	0.007	0.006	0.004	0.004	0.005	0.004	0.004
R7	0.006	0.005	0.003	0.003	0.004	0.004	0.004
R8	0.003	0.003	0.002	0.002	0.002	0.002	0.002
R9	0.002	0.002	0.001	0.001	0.002	0.001	0.001
R10	0.006	0.005	0.004	0.003	0.005	0.004	0.004
R11	0.003	0.003	0.002	0.002	0.003	0.002	0.002
R12	0.002	0.002	0.001	0.001	0.002	0.001	0.001
R13	0.006	0.005	0.003	0.003	0.004	0.004	0.004
R14	0.005	0.005	0.003	0.003	0.004	0.003	0.003
R15	0.007	0.006	0.004	0.004	0.005	0.005	0.005
R16	0.008	0.007	0.005	0.004	0.006	0.005	0.005
R17	0.007	0.007	0.004	0.004	0.006	0.005	0.005
R18	0.006	0.005	0.003	0.003	0.004	0.004	0.004
R19	0.005	0.005	0.003	0.003	0.004	0.004	0.003
R20	0.007	0.006	0.004	0.004	0.005	0.004	0.004
R21	0.002	0.002	0.001	0.001	0.002	0.001	0.001

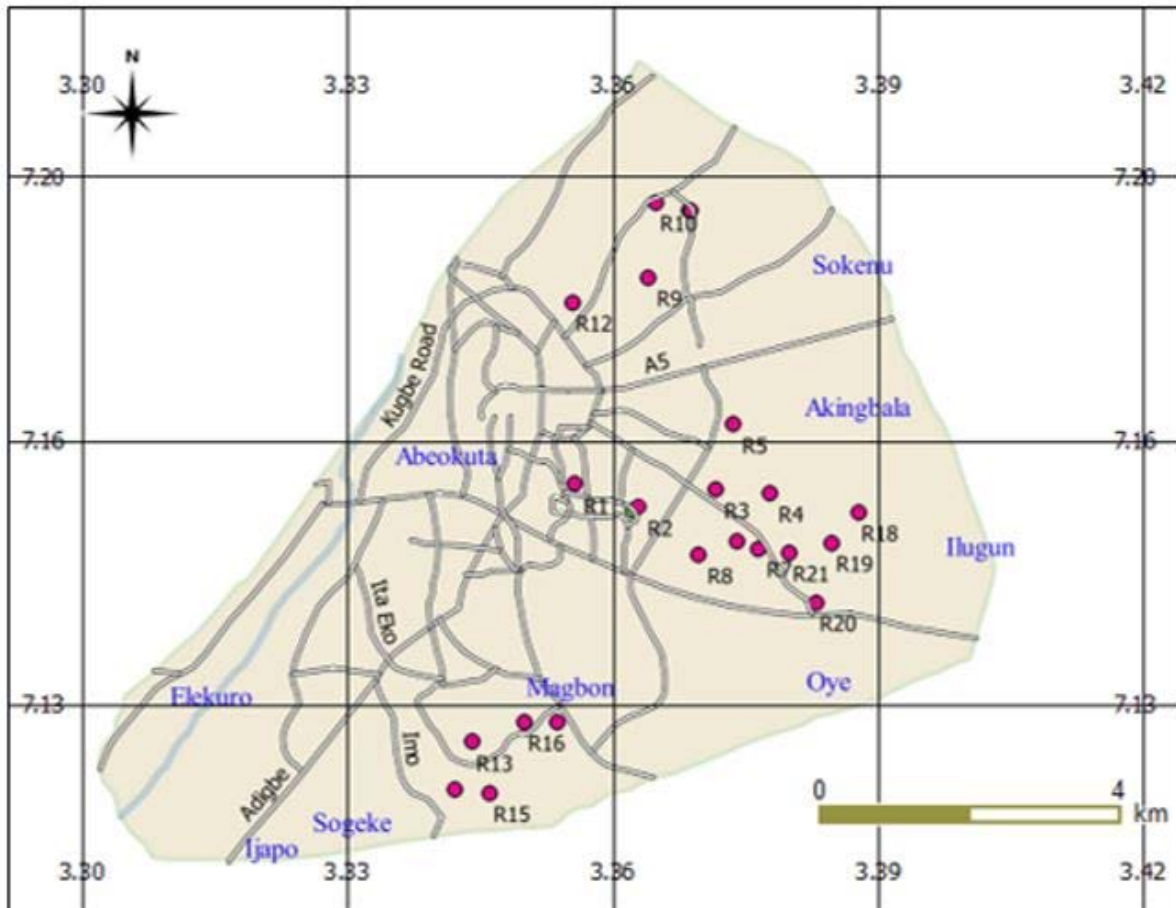
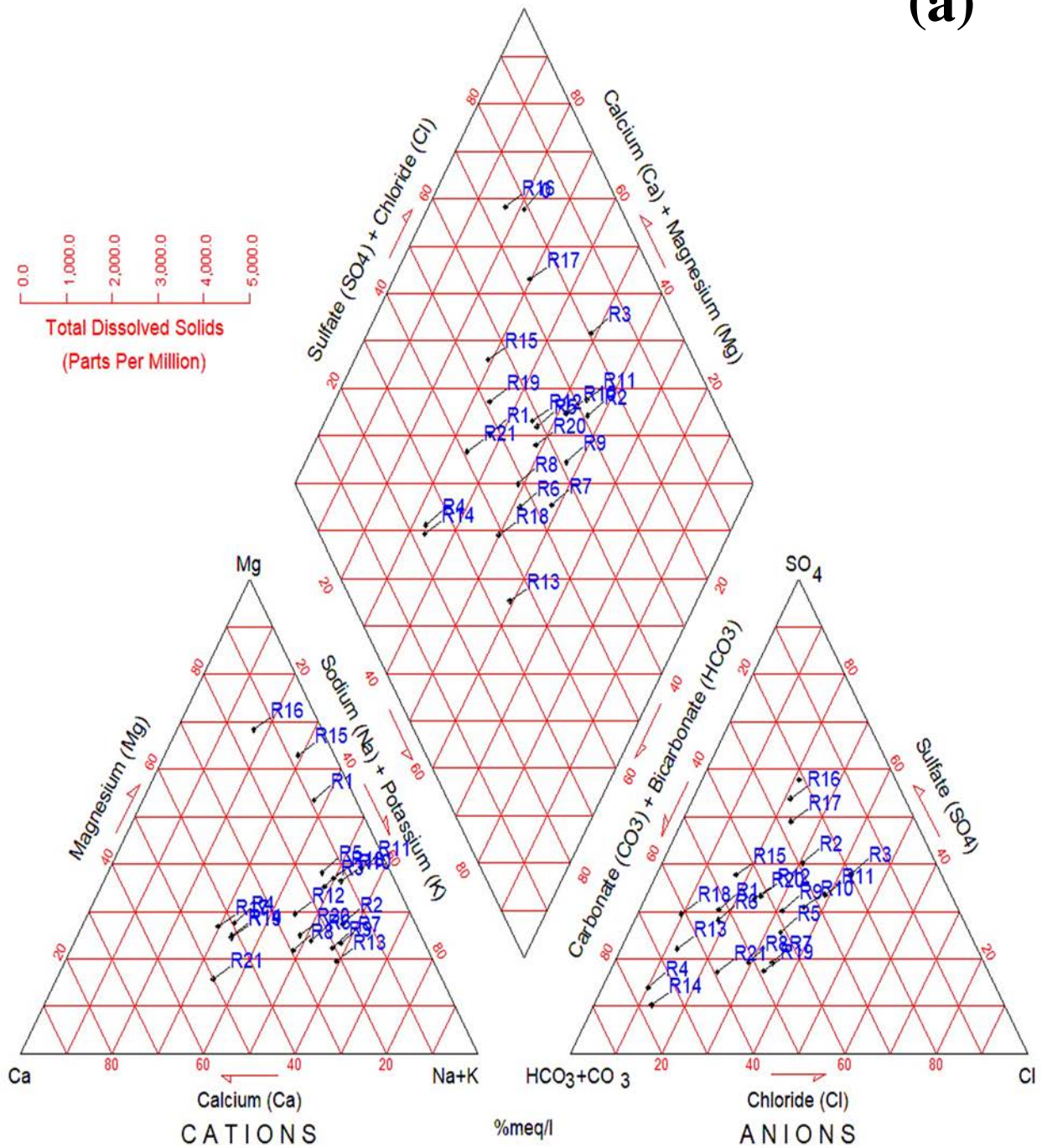


Fig. 1: Map of study area showing sampling locations

(a)



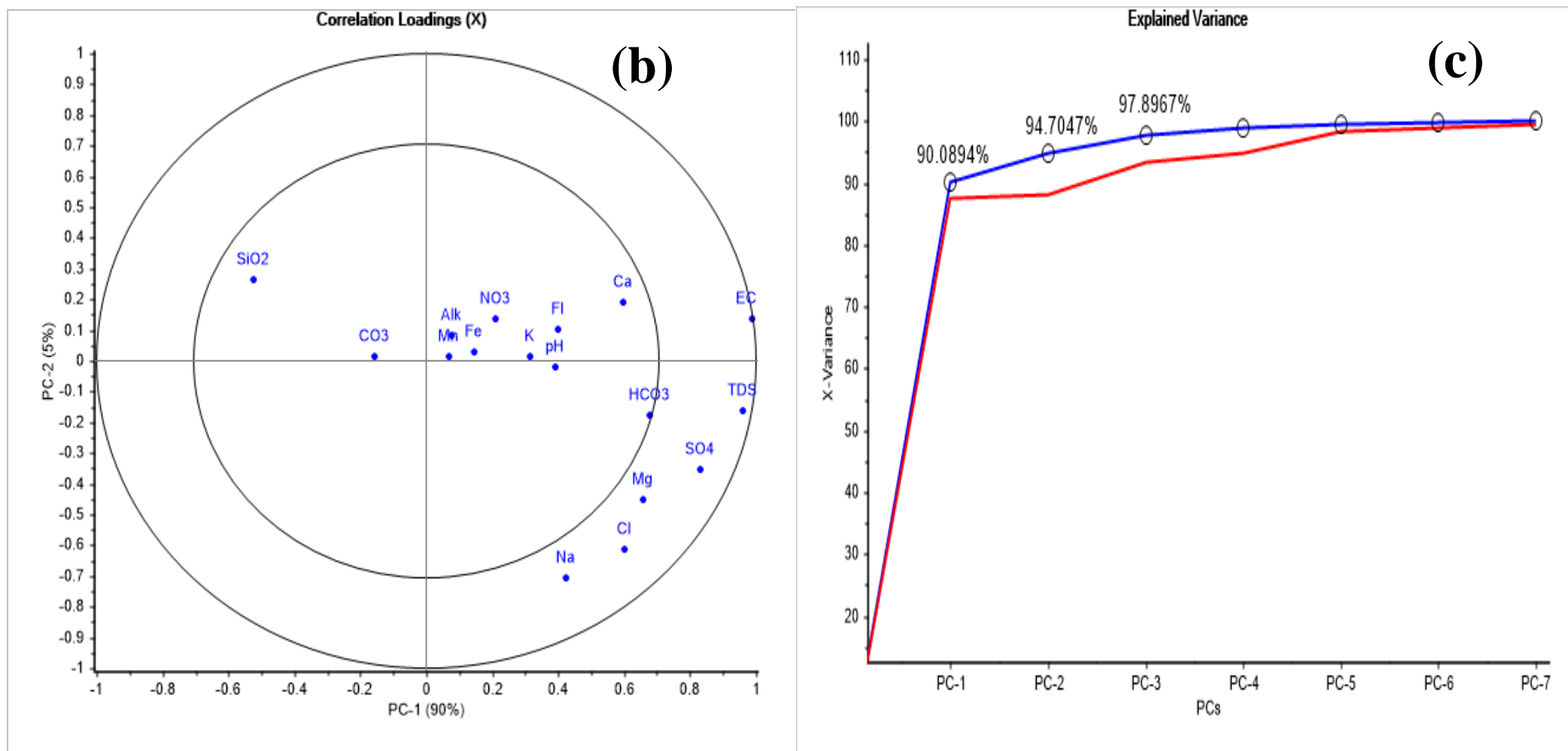
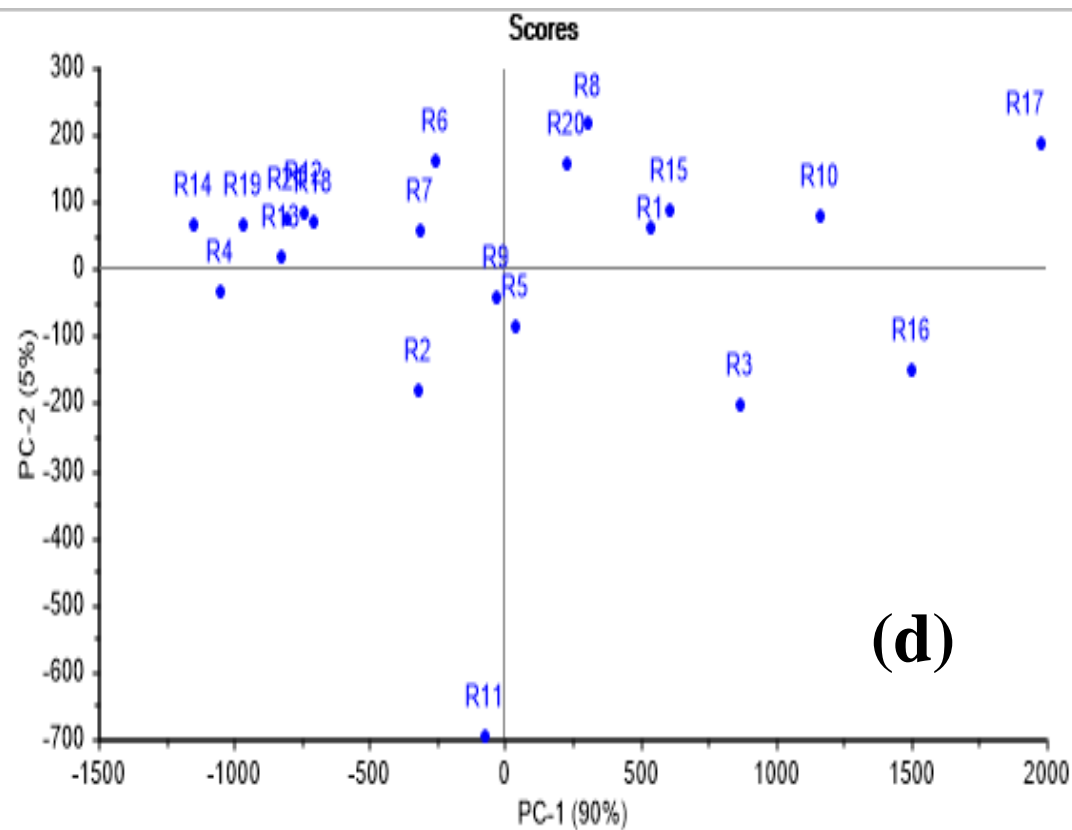
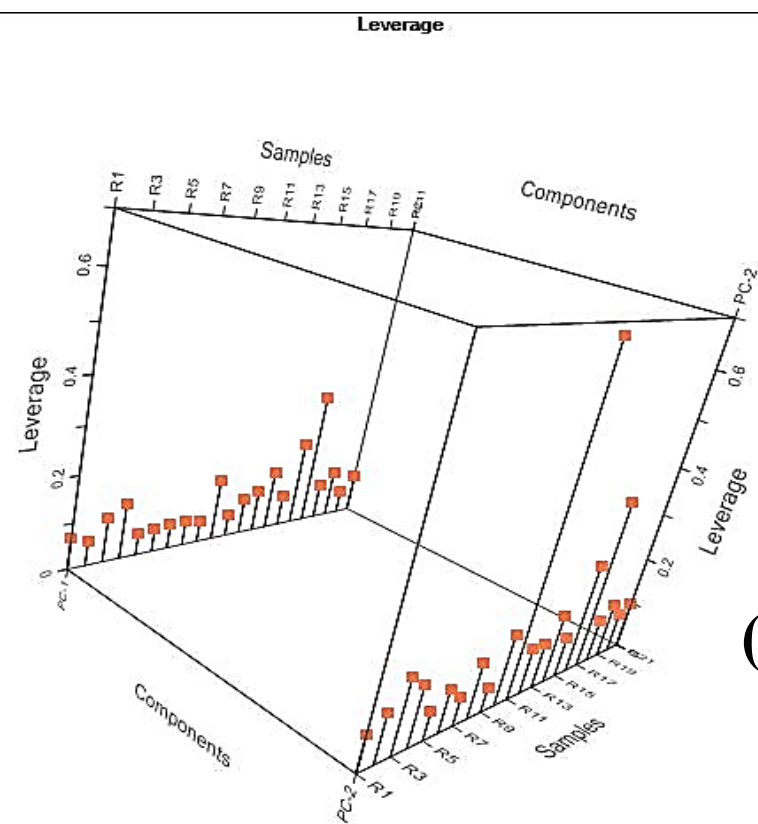


Fig. 2(a-c): (a) Characterization of hydrochemical facies with piper plot (b) PCA plot showing the loadings of each water quality parameter (c) Scree plot showing the percentage contribution of each principal component

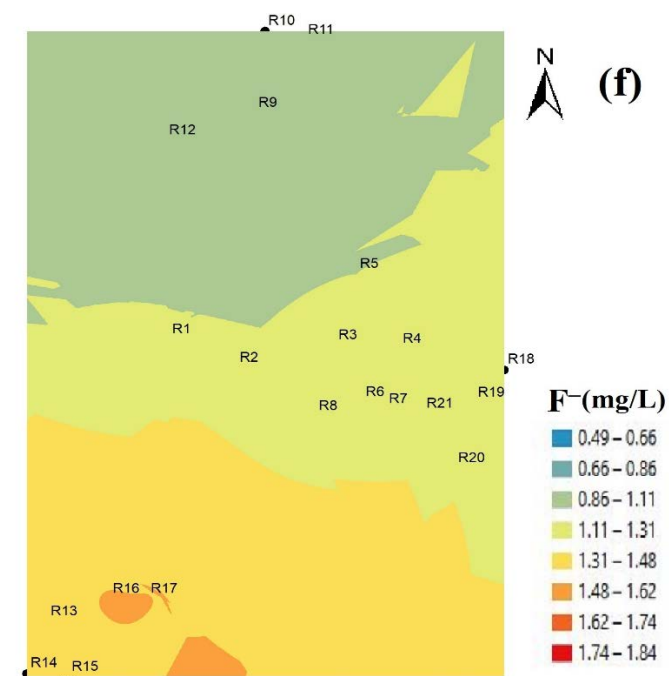
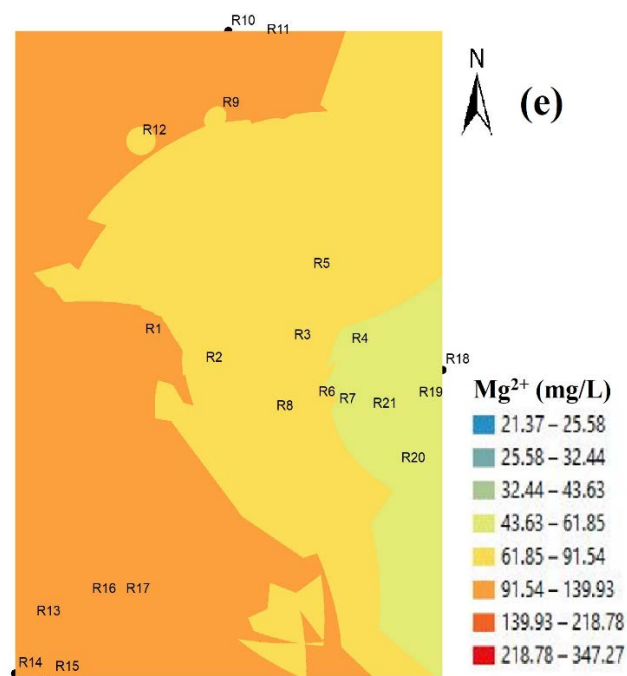
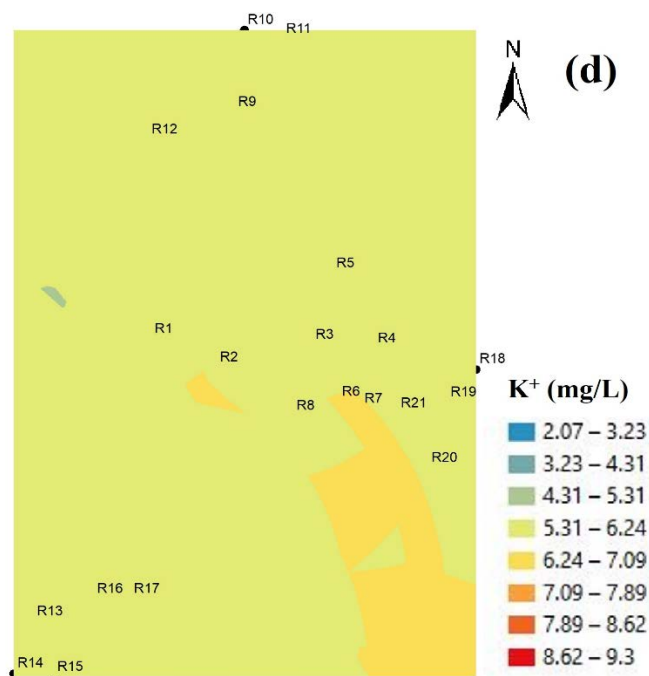
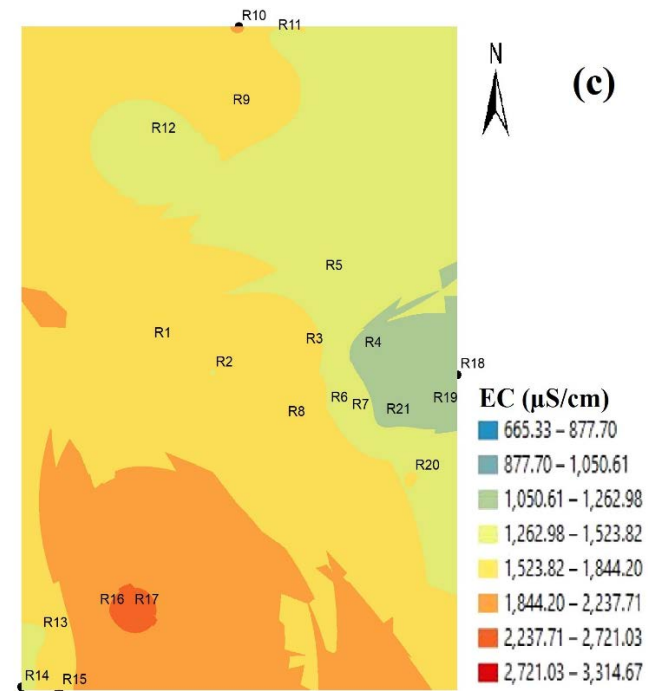
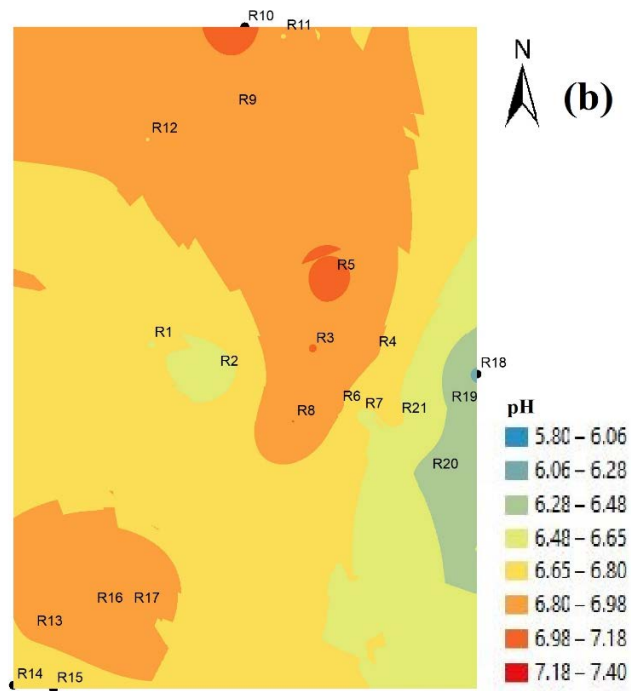
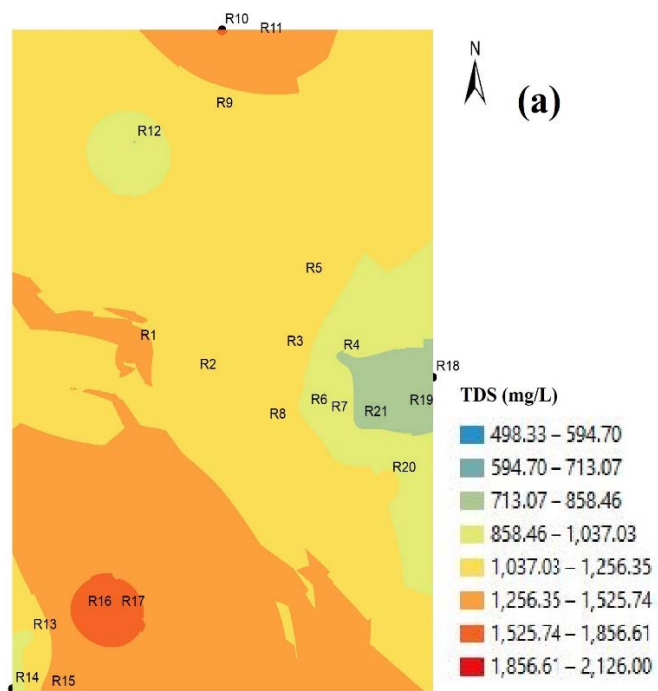


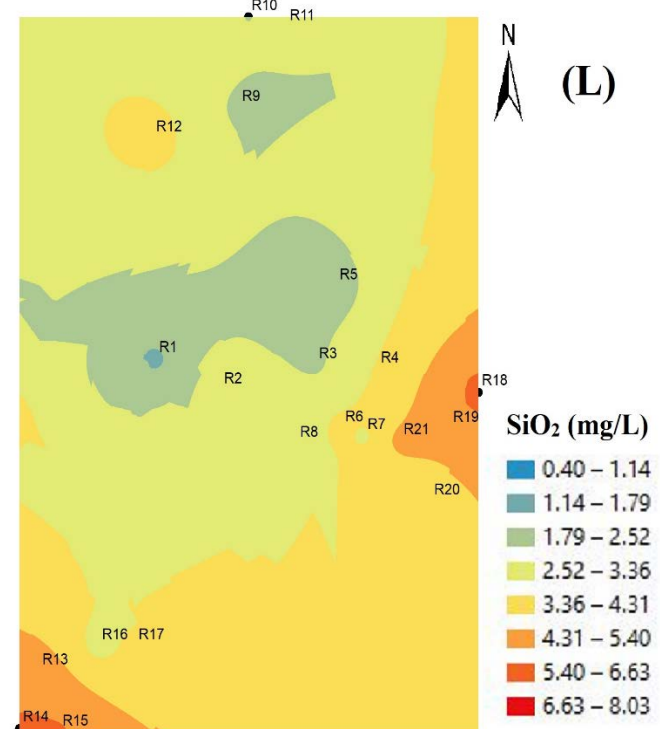
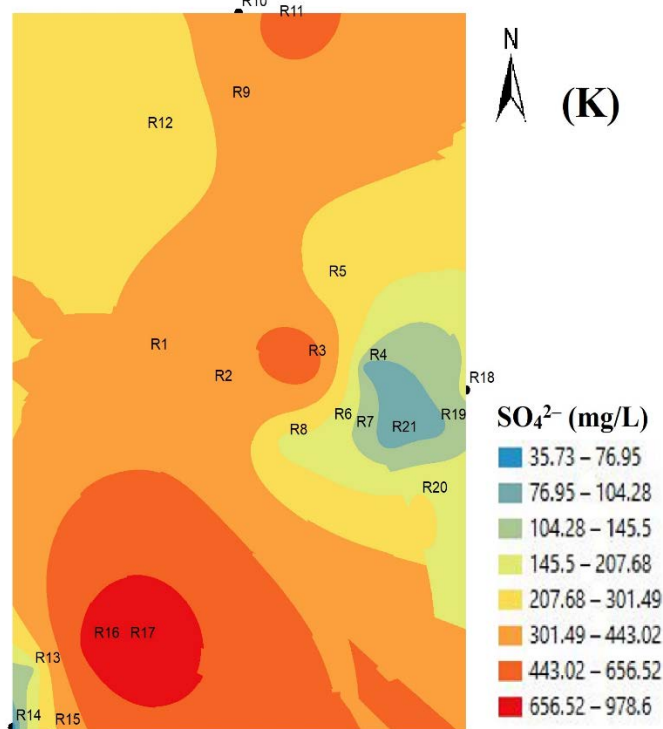
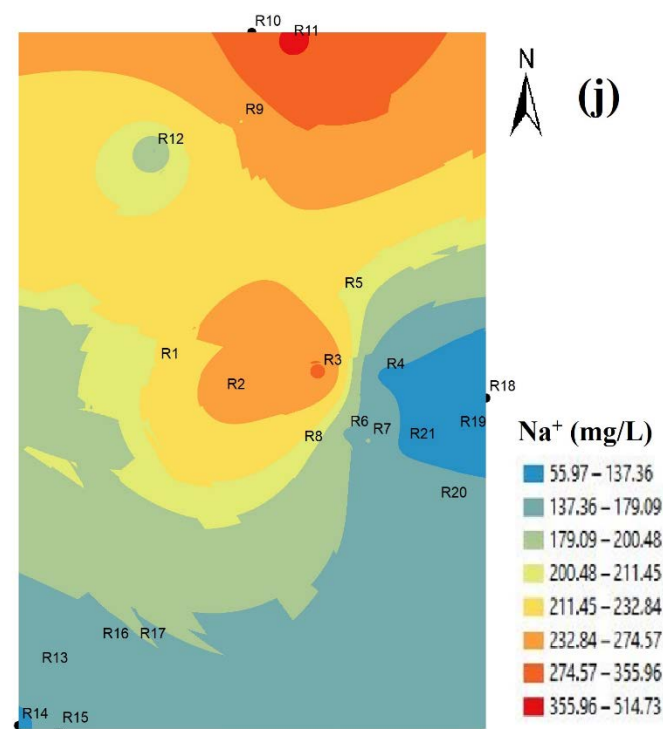
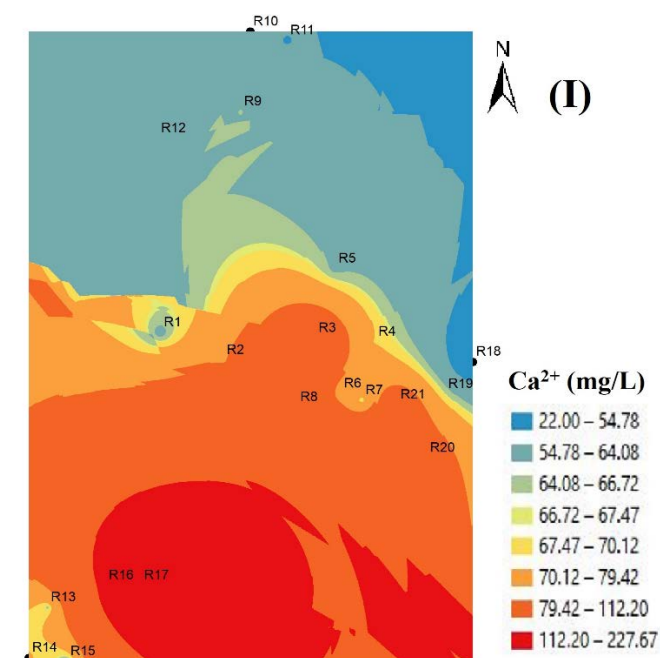
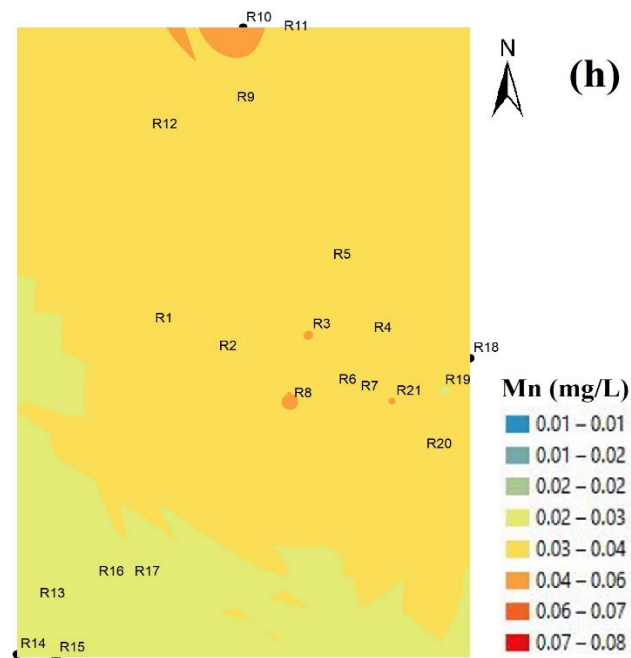
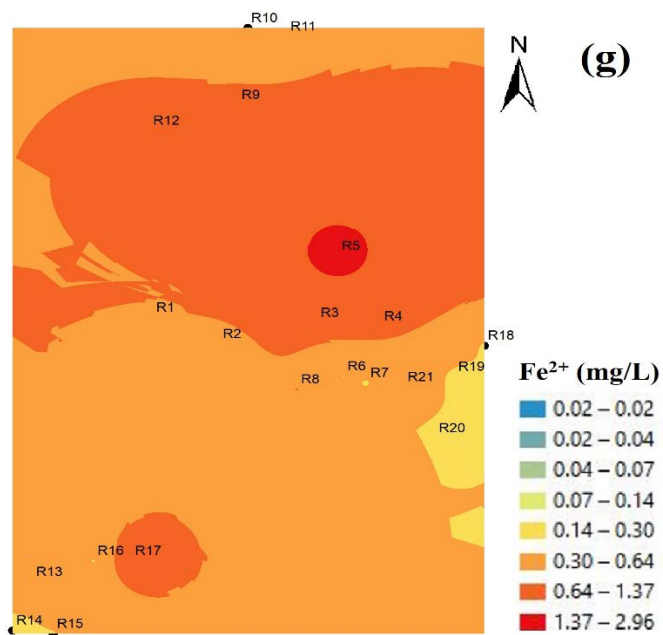
(d)



(e)

Fig. 2(d–e): (d) Score plot of the water samples (e) Influence plot showing the contribution of the water sample to the principal components





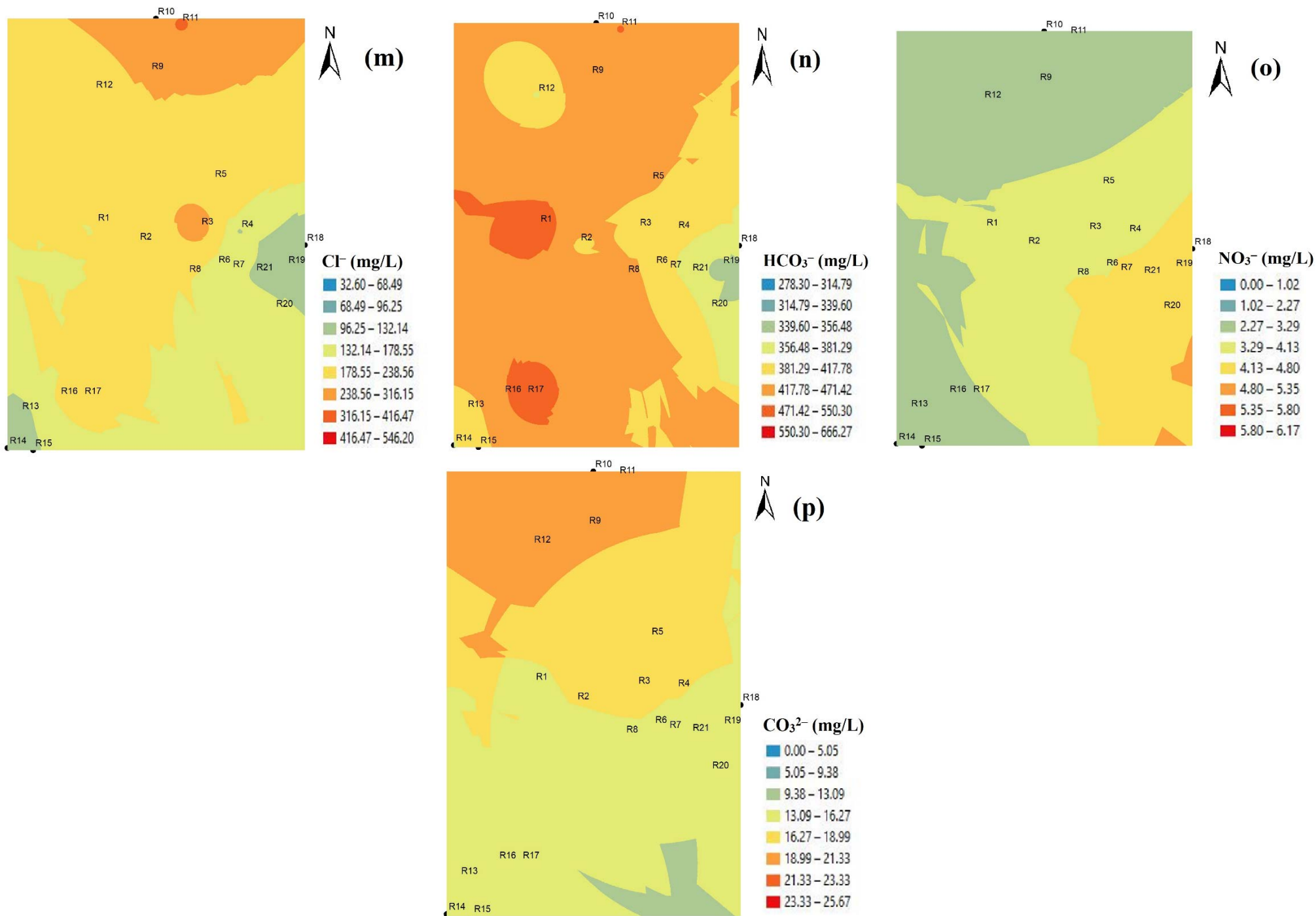
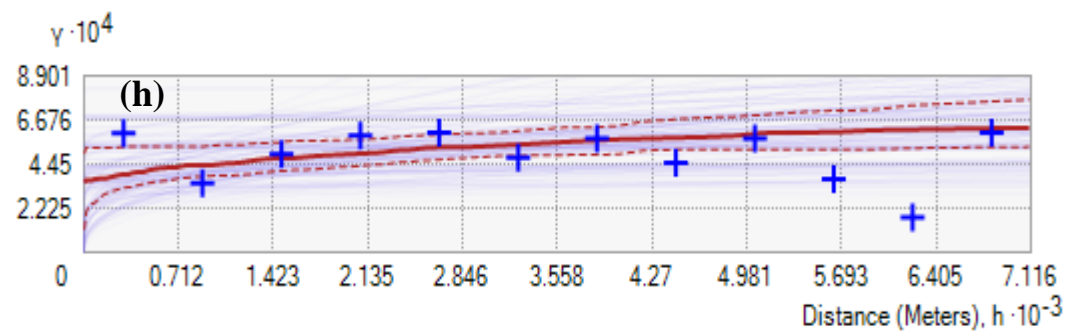
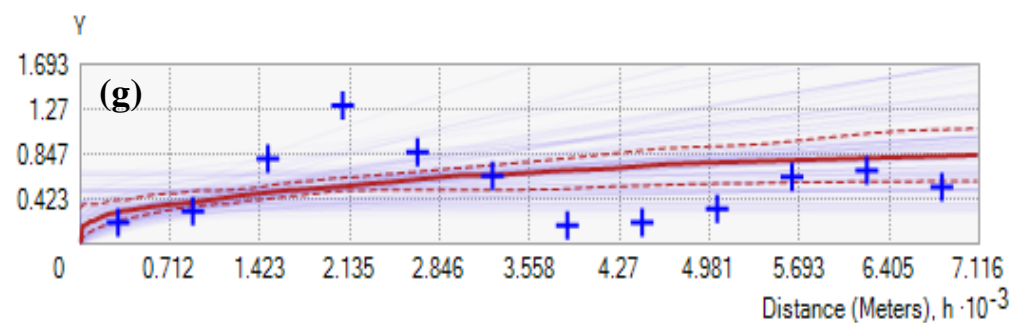
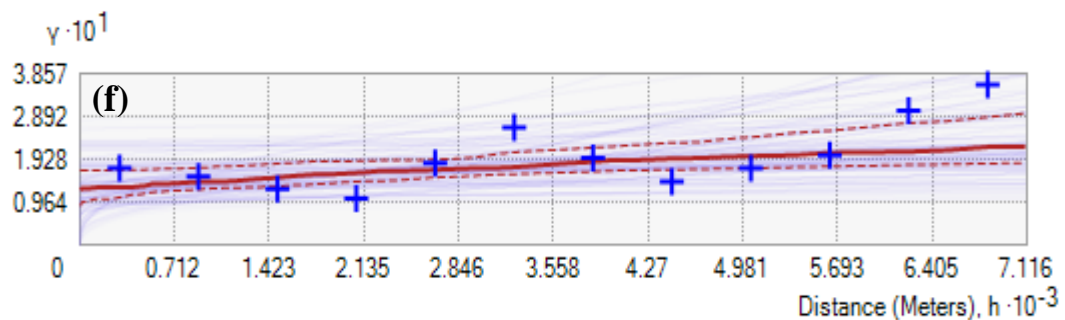
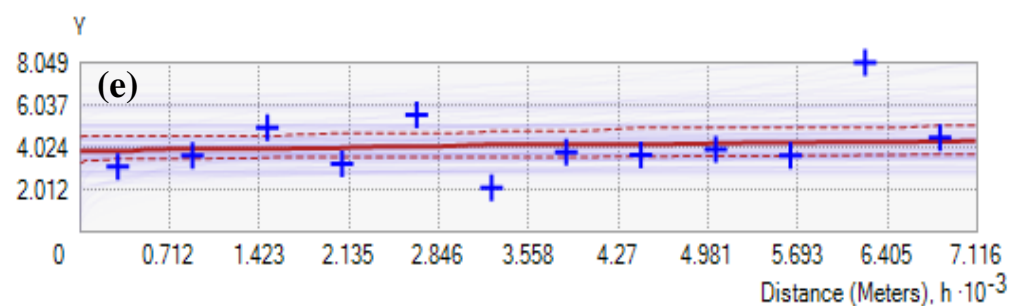
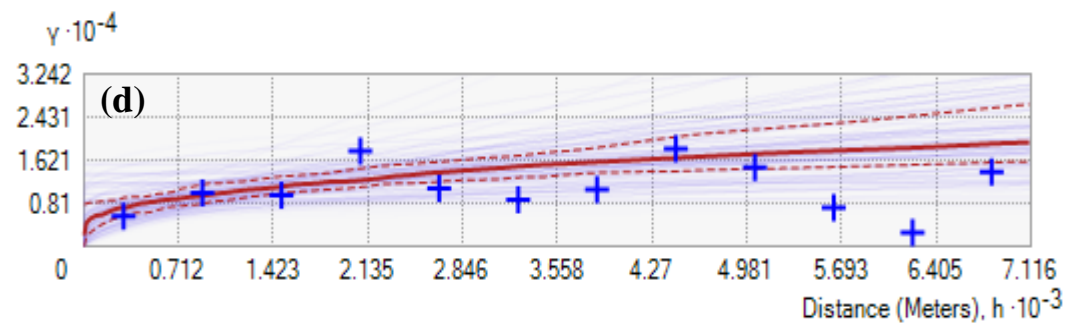
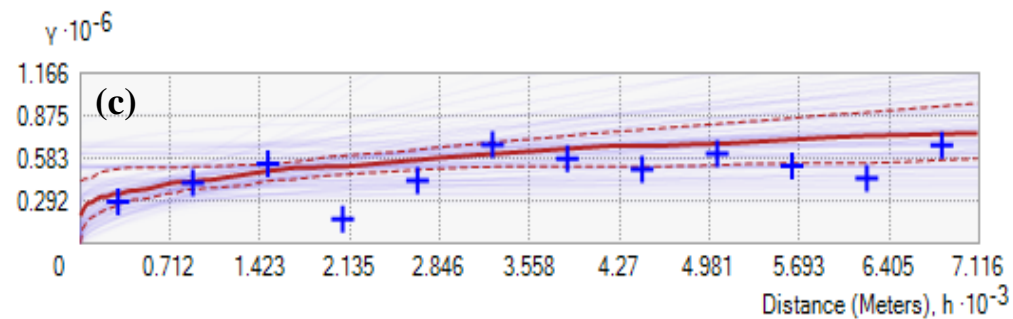
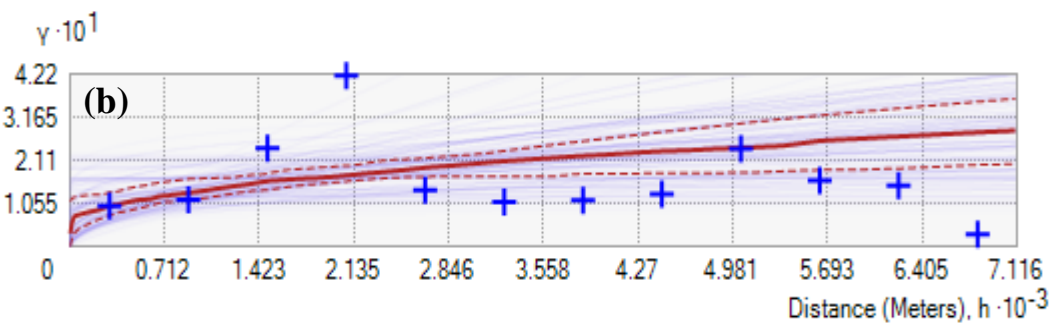
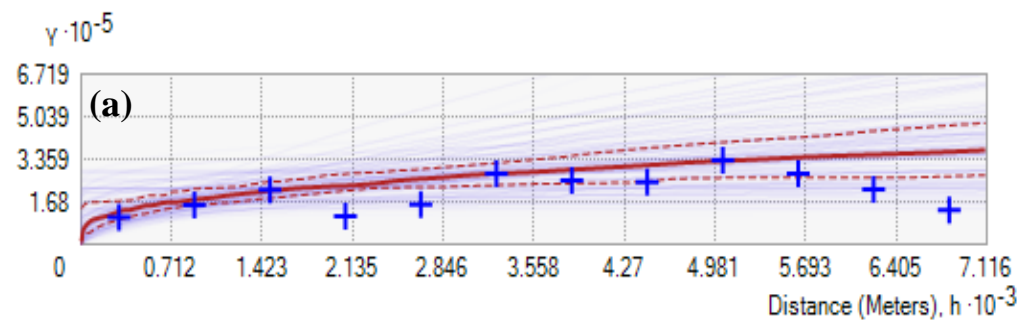


Fig. 3 : Spatial distribution maps of (a) TDS (b) pH (c) EC (d) K⁺ (e) Mg²⁺ (f) F⁻ (g) Fe²⁺ (h) Mn (i) Ca²⁺ (j) Na⁺ (k) SO₄²⁻ (l) SiO₂ (m) Cl⁻ (n) HCO₃⁻ (o) NO₃⁻ (p) CO₃²⁻ in the study area.



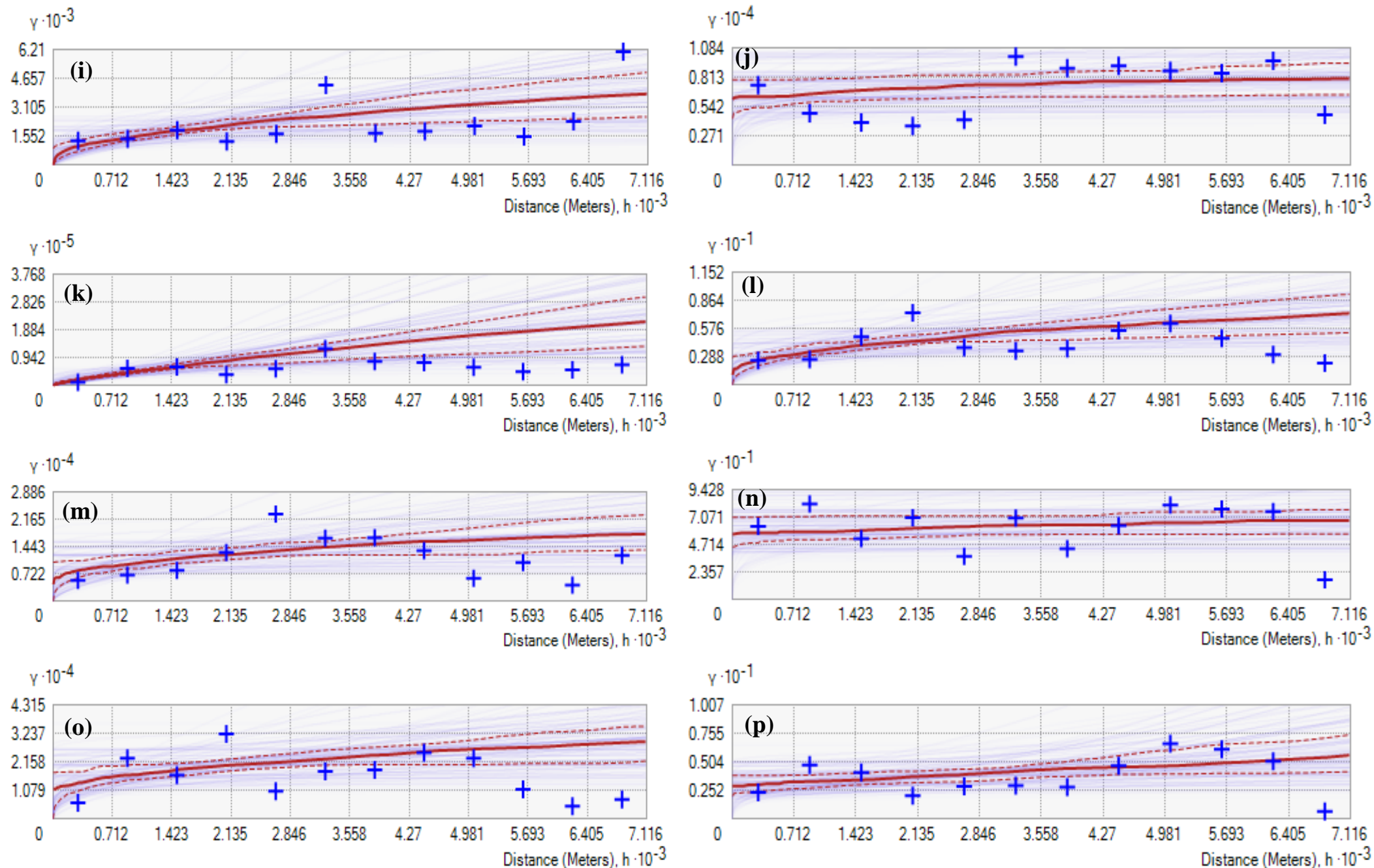


Fig. 4: Semivariograms of the water parameters (a) TDS (b) pH (c) EC (d) K^+ (e) Mg^{2+} (f) F^- (g) Fe^{2+} (h) Mn (i) Ca^{2+} (j) Na^+ (k) SO_4^{2-} (l) SiO_2 (m) Cl^- (n) HCO_3^- (o) NO_3^- (p) CO_3^{2-}

HIGHLIGHTS

- Water quality was assessed and compared with WHO standards
- Water quality parameters is modelled spatially and statistically
- Contaminant sources were inferred using multivariate statistical technique
- Health risk assessment was computed through ingestion and dermal contact route

Fluoride contamination in groundwater sources in Southwestern Nigeria: Assessment using multivariate statistical approach and human health risk

Emenike, Chidozie PraiseGod

2018-04-03

Attribution-NonCommercial-NoDerivatives 4.0 International

Emenike CP, Tenebe IT, Jarvis P. (2018) Fluoride contamination in groundwater sources in Southwestern Nigeria: Assessment using multivariate statistical approach and human health risk. *Ecotoxicology and Environmental Safety*, Volume 156, July 2018, pp. 391-402

<https://doi.org/10.1016/j.ecoenv.2018.03.022>

Downloaded from CERES Research Repository, Cranfield University